DEVELOPMENT OF A SPEED STABILIZER FOR RAPID SYNCHRONIZATION OF MINI-HYDRO GENERATOR

A dissertation submitted to the
Department of Electrical Engineering, University of Moratuwa
in partial fulfillment of the requirements for the
Degree of Master of Science

by

D.G. Subasinghe

Supervised by

Dr. J.P. Karunadasa

Department of Electrical Engineering
University of Moratuwa,
Sri Lanka

January 2009

DECLARATION

The work submitted in this dissertation is the result of my own investigation, except where otherwise stated.

It has not already been accepted for any degree, and is also not being concurrently submitted for any other degree.

UOM Verified Signature

D.G. Subasinghe

I endorse the declaration by the candidate.

Dr. J.P. Karunadasa

ABSTRACT

The objective of this study is to develop a damping method to stabilize the speed of the generator rotor during synchronization so as to minimize synchronization time and also to develop a prototype circuitry for a selected Mini-Hydro plant to obtain actual results.

The present system of the identified Mini-Hydro generator was modeled reasonably to identify the present response of the system for a step input. This was then simulated in Matlab and based on that a new PI controller with a power electronic switching circuit was developed to impart a resistive loading to generator in order to control the oscillation of the rotor during synchronization. Two switching strategies are discussed and they were tested at site for actual results.

One of the switching strategies showed positive results where the controller's performance is mostly in line with the simulated results.

ACKNOWLEDGEMENT

First I pay my sincere gratitude to Dr. J.P. Karunadasa who encouraged and guided me to conduct this research and on perpetration of final dissertation.

I make this opportunity to extend my thanks to Dr. Narenda De Silva for the valuable instructions given to me during the project.

I would like to take this opportunity to extend my sincere thanks to Mr. Prabath Wickramasinghe (Head-Industrial Solutions - Hayleys Ltd), Mr. Sudharshana Gamage (Electrical Engineer - Hayleys Ltd), Mr. M.G.K. Jayathunga (Superintendent – Gomala Oya (Pvt) Ltd) and his staff, Mr. D.U. Jayasooriya (Electrical Engineer - Ceylon Electricity Board) and his staff, Mr. A. Weerarathne (Electrical Engineer – Orient Electric (Pvt) Ltd), Nalaka Samarakoon (Executive- Orient Electric (Pvt) Ltd), W.A. Wijesiri (Electrical Engineer – Colombo Dockyard Ltd), R. Ranasinghe (General Manager – Orient Mag Line (Pvt) Ltd) and his staff, P.B.S.K. Baduwasam (Electrical Engineer – Micro Cells Ltd), who gave their co-operation to conduct the research and to develop the Prototype design successfully.

It is a great pleasure to remember the kind cooperation extended by the colleagues in the post graduate programme, friends, my subordinates in the office and especially my wife who helped me to continue the studies from start to end. Finally, I should also admire the patience of my beloved two kids during the project.

CONTENTS

List of tables

List of figures

Chapter 1

Introduction

1.1 Background

In Sri Lanka there are about sixty five numbers of Mini-Hydro power generators running at present. The plant capacities referred to Mini-Hydro range varies from 0.5 MW to 10 MW depending on the rainfall in the catchments area and average flow in the stream.

In the present context of high inflation of Thermal energy prices and with the influence of minimizing emission of green house gases, (GHGs) Mini-Hydro power generation plays a vital role as an alternative means of renewable energy. The Table 1.0 gives the details of the present and future plants expected to be connected with the grid.

Table 1.0 – Present status of the Mini-Hydro Projects in Sri Lanka.

Status of the Mini-Hydro Projects		
Mini Hydro Plants	No of Projects	Capacity (MW)
Presently in Operation	62	124.104
SPPA Signed Projects	32	77.860
Projects, SPPA to be Signed	20	34.605
LOI issued projects	53	87.905
Total anticipated By 2011	167	**324.474**

1.2 Hydro Electric Plant Schemes

There are three main types of hydroelectric plant arrangements, classified according to the method of controlling the hydraulic flow at the site.

1. Run-of-the-river plants, having small amounts of water storage and thus little control of the flow through the plant. Typically, most of the Mini-Hydro generator installations are of this system where they do not include a dam.
2. Storage Plants, having ability to store water and thus control the flow through the plant on a daily or seasonal basis. Larger hydro plants above 10MW capacity range are typically of this type.
3. Pumped storage plants, in which the direction of rotation of the turbine

is reversed during off peak hours, pumping water from a lower reservoir to an upper reservoir, thus 'storing energy' for later production of electricity during peak hours. However, this scheme of hydro plant installations are not yet set up in Sri Lanka.

1.3 Frequency of shutdowns of a Mini-Hydro Generator

The power is generated at low voltage level of 400/415 Volts and is stepped up by a step-up transformer to connect with the grid at distribution level voltage of 33 kV. The length of the electricity transmission line from the plant's transformer and all the way up to the load Bus at distribution network may be a few tens of kilometers and in most of the cases it is passing through the forest via overhead lines.

There are several causes that may affect a Mini-Hydro generator to shut down whilst in operation. They can be outlined as, the earth faults in the electricity lines (mainly tree leaves touching the transmission lines), lightning, planned and unplanned interruptions in that particular area connecting to the load bus of the distribution network and for maintenance of the plant itself. The Table 1.1 provides details of number of shut downs over year 2008 of a selected plant 'Gomala Oya' at Parakaduwa, Eheliyagoda. (1 MW plant capacity)

Table 1.1- Details of number of shutdowns of the selected Mini-Hydro plant.

Calendar Year	Number of Shutdowns
2008 (Jan to Dec)	48

1.4 Synchronizing of a Mini-Hydro Generator with the Grid

To resume power export to the grid after a shutdown will require generator to synchronize with the grid supply. This can be done either by fully automatically with the use of a PLC control system or by manually. In either process, the Hydro Turbine should be ramped up to the near synchronous speed at a rate decided by the Governor, Turbine and Penstock characteristics. Then the terminal voltage and Phase angle have to be adjusted to match with those of grid parameters before closing the Generator breaker.

The time taken for rotor speed ramping will typically be in the range of 3-4 minutes and then generator synchronizing would take another 2-5 minutes depending on the plant design. Figure 1.0 shows a graph of a speed Vs time during a typical synchronization process.

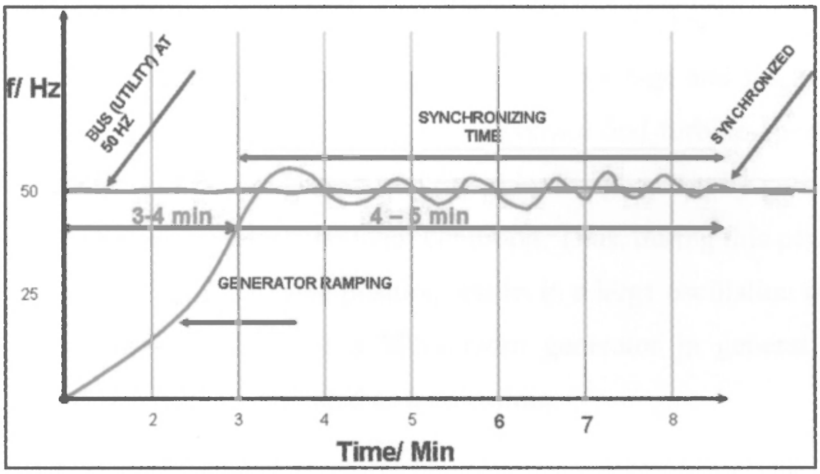

Figure 1.0 – Graph of a typical Generator speed Vs Time during Synchronization.

1.4.1 Ramping Period

During the ramping period the Inlet valve (wicket gates for Francis and Kaplan turbines, runner blades for Kaplan turbines, and Nozzle jets for Pelton Turbines) starts to open in steps so that hydro turbine starts receiving Hydro energy to gradually accelerate the speed from the stationary position. The rate of acceleration of the speed has limitations and is characterized by the Penstock characteristics. The ramping period considered here is the time taken by the generator to ramp up from stationary state up to 95% of the rated speed (or 95% of the rated frequency, which is 47.5Hz)

1.4.2 Synchronizing Period

During this process, the Synchronizer takes the control of the governor and gives biasing signals to raise or lower the speed of the rotor to synchronize with the bus frequency and to match the phase angle (if it is in Auto mode). Synchronization begins just at the end of Ramping (approximately 47.5Hz) and the synchronizing time is the time between the end point of ramping and the point of closing the generator breaker after synchronization. (at 50 Hz after matching with grid frequency and phase angle). Once the breaker is closed, the synchronizer is switched off and PLC controller will take control over the speed and generator loading. The PLC controller has the function of ALC (Automatic Loading Control) which will set the load reference point depending on the water level in the fore bay tank.

1.4.2.1 Downtime during Synchronization Period

Synchronization period of a Mini-Hydro generator is highly volatile. This time can be positively influenced by the stability of the grid Voltage and frequency at the time of attempting synchronization and by the governor and turbine characteristics. The spinning of heavily massed rotor is controlled by the governor by controlling the water flow in to the turbine under 'no load' condition. Thus, during this period even a small step increase of the inlet valve position results in a large oscillation of the rotor speed. Therefore, synchronizing of a Mini-Hydro generator in general is a time consuming exercise which is accounted as a downtime.

1.4.2.2 Loss of Energy Production during Synchronizing Period

Most of the Mini-Hydro installations are run-of-the-river type (not storage type) and therefore the amount of power generated at a given time depends on flow level of the stream and availability of the water in the fore bay tank. Therefore the loss of energy production during a downtime cannot be fully recovered later by increasing the generator load factor. This is a disadvantage of run-of-the-river type plants where there is only a small amount of energy storage capability in the set up. As indicated in Table 1.1, since the number of shutdowns are substantial, the total accumulated downtime during synchronization over a year would cause a considerable production loss.

1.4.3 Importance of Minimizing the Synchronization Period

Even though the Ramping Period is constrained by the design of the plant itself, minimization of synchronization Period is an alternative to minimize the total downtime. Further as per the Figure 1.0 the synchronization period is generally longer than ramping period. Therefore, there is a potential to minimize the total downtime by approximately 25-50% by optimizing the synchronization time.

1.4.4 Impact on the Present Design of the Plant

In order to make the project viable and to obtain the management's approval for practical implementation, it is a requirement that the new circuit development should not have any interference on the present system. Therefore, the function of the new controller has to be totally independent while improving the performance of the present system. Further, once it is disconnected (switched off) the system should turn back to its original set up.

1.5 Motivation

Minimizing the synchronization time of a Mini-Hydro generator, will enhance the operating characteristics of fast response for start-up and also will produce additional units of energy due to reduced downtime. The anticipated outcome in terms of additional revenue would be considerable for a plant operator.

As an Engineer with a background of installation and commissioning of standby diesel power generators, application and commissioning of generator synchronizing and load management systems in the industry, the author selected this topic to investigate the possibility to enhance the synchronization process of Mini-Hydro Generators.

Chapter 2

Problem statement

2.1. Identification of the Problem

The expectation of this project is to reduce the down time of the synchronization process since it finally affects the total revenue that can be generated from the plant. This needs to be analyzed by exploring the possibilities for stabilizing the rotor speed during synchronization. This will require development of a new control system, which should facilitate the synchronizing function of the existing synchronizer while it is not interfering with the installed control set up. The design of the new controller involves modeling of the Mini-Hydro plant, use of Matlab and control theory for designing of LTI control systems in S plane and also Digital Control principles for practical implementation of control algorithm in a microcontroller unit (MCU). The following areas need to be focused.

1. How to model the system during Synchronization?
2. What hardware components to be sourced and what to be produced to make the prototype design?
3. Programming the microprocessor according to the control algorithms.
4. How to obtain experimental results?

2.2. Objective of the Project

The expectation of this project is to explore alternative methods that can be applied for damping the rotor so that it could stabilize at a reference input (bus frequency) and for more to develop a prototype circuitry for a selected Mini-Hydro plant for real life testing of the concept. Damping the system should be done by electrical means in a controlled manner so that the rotor speed can be stabilized within a desired time.

The design of the new controller involves identifying the model of the present system and model development of the proposed new controller. The model has to be analyzed in Matlab simulation which will require transfer function of the system in S plane and also Digital Control principles for practical implementation of the control algorithm in Z plane. During the investigation more attention is paid on the followings,

A) Modeling of the identified Mini-Hydro plant (present system)

1. Derive differential equations for power equilibrium. Moreover, derive close loop transfer function of the present system.
2. Find out the viscous frictional damping of the generator assembly.
3. Estimation of PID values of the present synchronizer using Matlab

B) Identify the viable options for applying resistive loading to the system for damping

1. Inertia calculations to identify range of power requirement for damping the system during a desired time frame.
2. Selection of Power Electronic Devices for optimum performance of the circuit.
3. Programming the Microprocessor for control algorithm.

C) Identify a suitable model plant and to obtain plant owner's permission for testing the circuitry at site to get experimental results.

2.3 Importance of the Project

As outlined in the previous chapter, there are several causes that may affect a Mini-Hydro generator to shut down whilst in operation. They may be due to temporary line faults and power interruptions at the receiving end as well as for planned shutdowns. The plant should be able to resume power generation within a shortest time period possible when it is required to set the unit back in operation. Therefore, development of a Speed stabilizer is important to minimize the synchronization period.

This research will help to explore the feasible solutions for damping the rotor during synchronization and thereby to achieve rapid synchronization. The prototype development of the proposed controller and testing it with an identified model plant can obtain real life experimental results. The results can then be ascertained for commercial viability for the benefit of relevant industry.

Chapter 3

System Modeling

3.1. Introduction

For the success of new circuit development, it is required to select a suitable site to obtain more information to understand the operation of the Hydro Power plant system and also to obtain experimental results from the prototype design. Hence, it was decided to locate a model site with easy access from Colombo. The Figure 3.0 shows the selected plant for the project at Ehelliyagoda.

Figure 3.0 – 'Gomala Oya' Mini-Hydro Plant at Ehelliyagoda.

3.1.1 Details of Identified Mini-Hydro plant

Name:	Gomala Oya (Pvt) Ltd.
Location:	Parakaduwawa, Ehelliyagoda, 75Km from Colombo
Capacity:	1MW, 415V, 50Hz, 750RPM, 8 Pole, Synchronous Generator
Hydro Turbine:	Francis Turbine, with 12 Numbers Wicket Gates
Head:	100m
Commissioned:	May 2005

The information collected from the site are as given below,

- Datasheet of present synchronizer
- Datasheet of Governor

- Datasheet of Turbine
- Datasheet of the Alternator
- Historical records on the plant shutdowns

3.1.2 Initial Field Measurements

At the beginning of the project, in order to gather sufficient information regarding the 'settling' time of the generator rotor speed variation Vs time, a Power Analyzer reading was recorded during synchronization. The Figure 3.1 shows a graph of Frequency Vs time during synchronization.

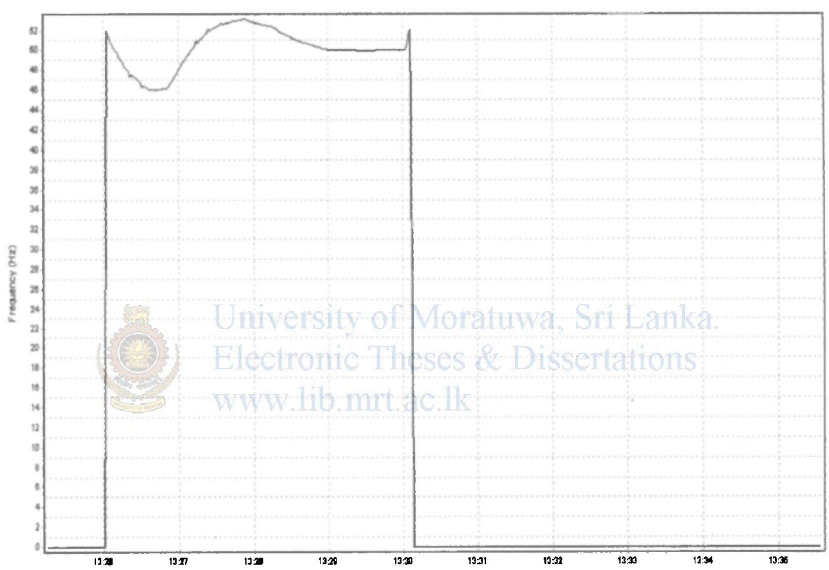

Figure 3.1 – Graph of Frequency Vs time during Synchronization.

3.2. Notation

J	Moment of Inertia of the Rotor Assembly in units	kgm^2
C	Viscous Damping Coefficient	kgm^2/sec
ω_s	Grid frequency converted to speed	rad/sec
ω	Speed of the Rotor	rad/sec
ω_0	Near synchronous speed at which system modeled	rad/sec
R	Governor speed Droop	%
T_G	Governor Time Constant	sec
T_H	Hydro Turbine Time Constant	sec
K_G	Governor Gain	-

E_L	Load Error signal to Governor	-
P_v	Change of Inlet Valve position	-
K_T	Absolute Power Gain from Turbine	-
P	Number of Poles of the Alternator	-
N_s	Synchronous speed of the Alternator	RPM
f	Cycle frequency of the Alternator	Hz
X_s	Synchronous reactance of the Alternator	H
R	Stator winding resistance	Ω
K,a,b	PID parameters of the present synchronizer	-
T_m	Torque excerted on Rotor by Turbine	Nm
T_L	Torque excerted on Rotor due to Load (grid)	Nm
P_m	Mechanical Power by Turbine	W
P_L	Power supplied to the Load (grid)	W
Te	Torque excerted on Rotor by Artificial Load	Nm
$\dot{\theta}$	Measured speed of Rotor	rad/sec
K_P,d	PI parameters of the new controller	-
Ke	Absolute Power Gain from Artificial Load	-
Pe	Electrical Power consumed by Artificial Load	W
S	Linear Time Invariant System in 'S' Plane	-
Z	Discrete System in 'Z' Plane	-

3.3. Model of the Present Mini-Hydro Generator

In order to develop the model of the present Mini-Hydro Generator plant, sub systems were identified and transfer functions of them were derived. Then the sub sytems were interconnected to develop the whole model. The major sub components involved in the model are synchronous Generator, Turbine, Governor and synchronizer.

The equation governing the rotor motion of the synchronous machine is based on the elementary principle in dynamics which states that accelerating torque is the product of the moment of inertia of the rotor times its angular acceleration. Since the viscous frictional damping is present in the rotor and turbine assembly, the torque balance of the synchronous machine can be written as depicted in 3.3.1.

3.3.1 Torque Equilibrium

When the generator is running at steady state, the torque balance of the system is written as,

$$J\ddot{\theta} + C\dot{\theta} = T_m - T_L$$

3.3.2 Power Equilibrium

When the rotor is spinning at near synchronous speed of the machine ω_0, the power equilibrium of the system is as follows,

$$J\omega_0\ddot{\theta} + C\omega_0\dot{\theta} = P_m - P_L$$

$$\dot{\theta} = \omega$$

$$J\omega_0\dot{\omega} + C\omega_0\omega = P_m - P_L$$

3.3.3 Laplase Transformation of Power Equilibrium

$$J\omega_0 s\omega(s) + C\omega_0\omega(s) = P_m(s) - P_L(s)$$

$$\omega(s) = \frac{P_m(s) - P_L(s)}{\omega_0(Js + C)}$$

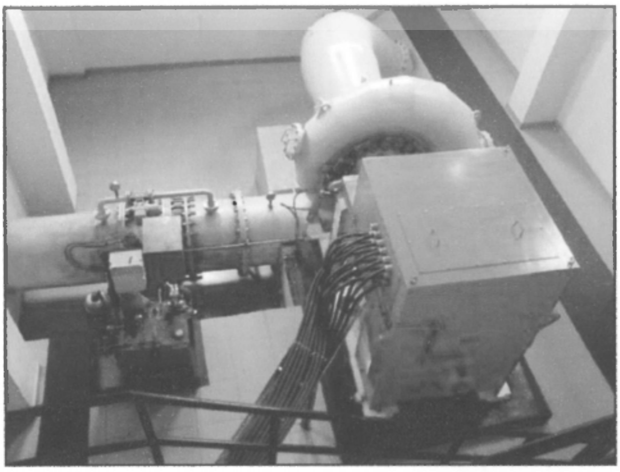

Figure 3.2 – A Picture of Governor, Francis Turbine and Generator.

3.3.4 Governor Model

The Governor system is the key element of the plant that controls speed and power. It consists of control and actuating equipment to regulate the flow of water through the turbine, for starting and stopping the unit, and for regulating the speed and power output of the turbine generator. The governor system includes set point and sensing equipment for speed, power and actuator position, compensation circuits, and hydraulic power actuators, which convert governor control, signals the mechanical movements of the wicket gates. (wicket gates for Francis and Kaplan turbines, runner blades for Kaplan turbines, and Nozzle jets for Pelton Turbines). The hydraulic power actuator system includes high-pressure oil pumps, pressure tanks, oil sump, actuating valves and servomotors.

Older governors are of the mechanical-hydraulic type, consists of ballhead mechanical dashpot and compensation, gate limit and speed droop adjustment. Modern governors are of electro-hydraulic type where the majority of the sensing, compensation and control functions are performed by electronic and microprocessor circuits. Compensation circuits utilize Proportional plus Integral plus Derivative controllers to compensate for the phase lags in the turbine-generator-governor control loop. The governor that is used in the identified plant is an electro-hydraulic type and the model of same is given below.

$$P_V(s) = \frac{K_G E_L(s)}{(1+sT_G)}$$

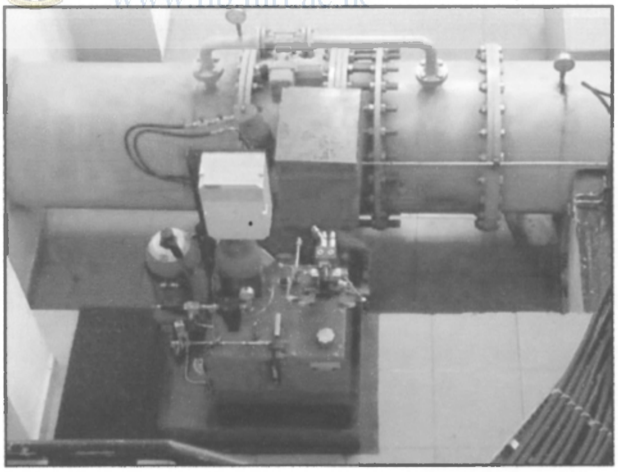

Figure 3.3 – A picture of Hydraulic Governor (shown in color Blue).

3.3.5 Turbine Model

The type of Turbine selected for a particular application is influenced by the head and flow rate. There are two classifications of hydraulic turbines named as impulse and reaction. The impulse turbines are used for high heads-approximately 300m or greater. High velocity jets of water strike spoon shaped buckets on the runner, which is at atmospheric pressure. Impulse turbines may be mounted horizontally or vertically and include perpendicular jets (known as a Pelton.type), diagonal jets (known as a Turgo type), or cross-flow types.

In a reaction turbine, the water passes from a spiral casing through stationary radial guide vanes, through control gates and onto the runner blades at pressures above atmospheric. There are two categories of reaction turbines, Francis and propeller. In the Francis turbine, installed at heads up to approximately 360m, the water impacts the runner blades tangentially and exists axially. The identified Mini-Hydro plant is a Francis type with 100m head.

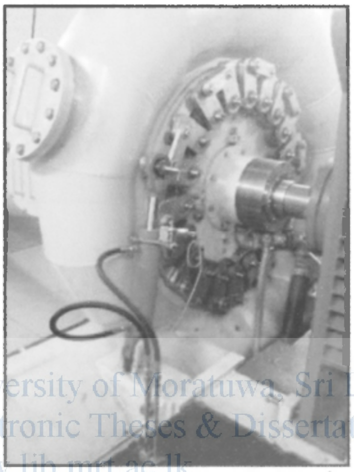

Figure 3.4 – A picture of Francis Turbine with 12 Wicket Gates

The Automatic Loading Control (ALC) of the plant is a PLC which provides load reference signal depending on the water level in the Forebay tank. This also maintains the optimum power dispatch of the plant where the load reference is varied to provide the optimum efficiency of the plant in a given period of time. The Governor Droop is a preset value which maintains the speed-droop characteristics in response to change of generator load. The Figure 3.5 shows the model of the present Mini-Hydro plant and the model of the turbine is as follows,

$$P_m(s) = \frac{K_T P_V(s)}{(1+sT_H)}$$

The flow through the Turbine is controlled by the wicket gates on reaction turbines and by needle nozzles on impulse turbines. A turbine intake valve (main valve) is used to isolate the turbine during shutdown and maintenance. This is also used to regulate the flow during synchronization (at no load condition). This is called as 'double regulatory' system where the main valve also a motor operated valve that is controlled by the plant's PLC.

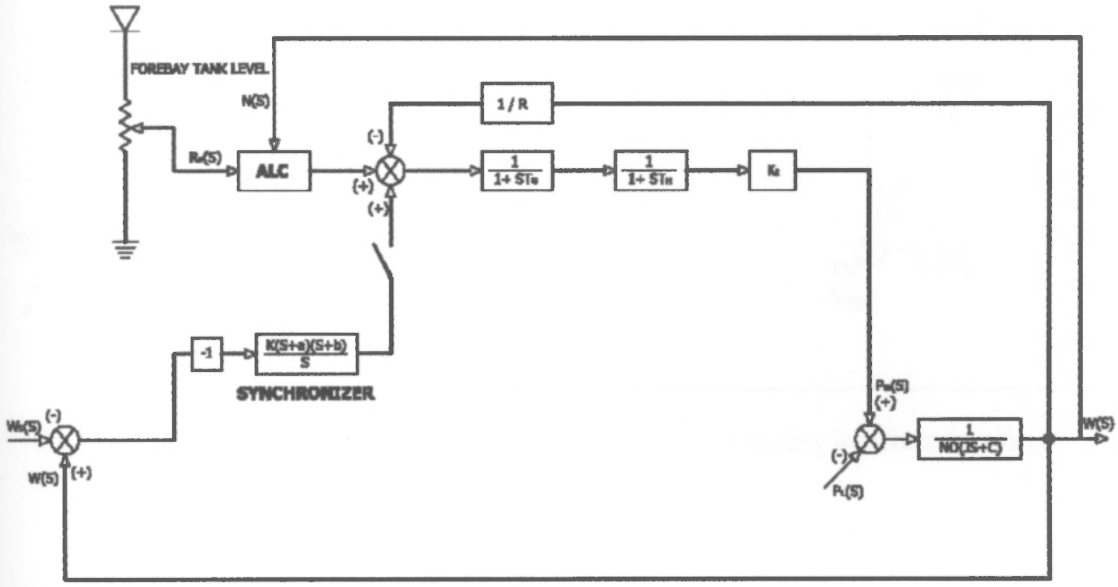

Figure 3.5 – Model of the present Mini-Hydro Generator.

3.4. Model of the Present Mini-Hydro Generator during Synchronization.

During the synchronization process the speed droop function and automatic loading control (ALC) are disabled and the speed control of the system will be governed by the Synchronizer. The generator breaker is in 'Open' position and therefore load is zero ($P_L(s)=0$). Synchronizer compares grid frequency against generator frequency and according to the error, PID controller in the synchronizer signals small step changes to Governor to increase or decrease generator speed. In order to formulate the model, the PID action of Synchronizer shall be expressed as follows,

$$\frac{K(s+a)(s+b)}{s}$$

Then the model during synchronization can be formed as shown in Figure 3.6.

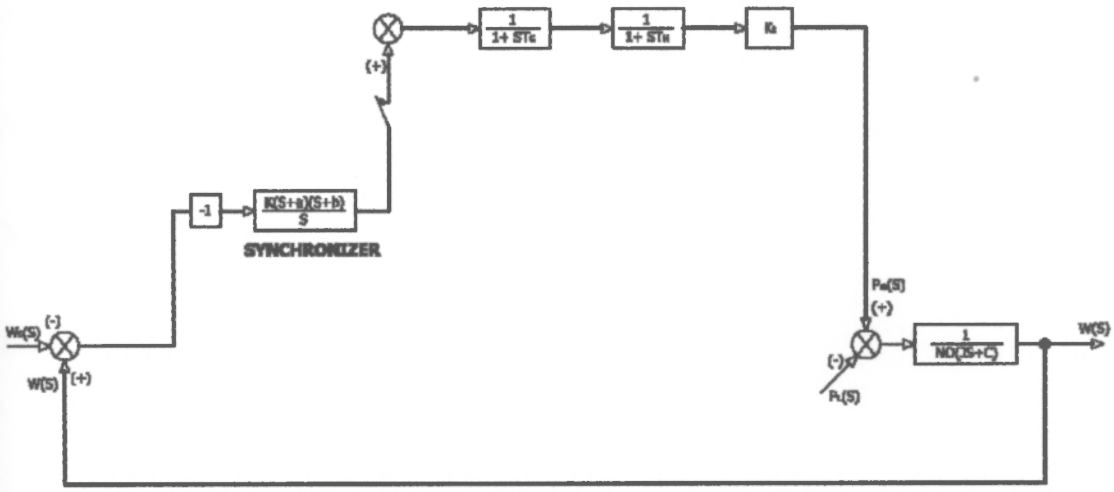

Figure 3.6 – Model of the present Mini-Hydro Generator during synchronization.

Figure 3.7 – A picture of the Automatic Synchronizer of the plant

3.4.1 Estimation of Model Parameters during Synchronization.

As shown in Figure 3.6, parameters involved in this model are K, a, b, T_G, T_H, K_T, P_m, ω, ω_s, J and C. In order to identify the present system during synchronization, these model parameters have to be derived or estimated using computational and experimental methods. At the summation block, $\omega(s)$ and $\omega_s(s)$ are measured quantities which are sensed from generator supply frequency and grid frequency respectively. Moment of inertia J and time constant values T_G and T_H are taken from manufacture's datasheets. Furthermore, K_T is estimated through inertia calculations where maximum possible value of P_m during Thus, PID values of the synchronizer can be then derived using Matlab.

3.4.2 Estimation of value for C

Since value of C is unknown it should be found experimentally. An equation is derived to find the value C by means of a differential equation for torque equilibrium.

When the Turbine gate is closed, $T_m = 0$. Then,

$$J\ddot{\theta} + C\dot{\theta} = 0$$

Laplace transform to solve differential equation,

$$J\left[s^2\theta(s) - s\theta(0) - \dot{\theta}(0)\right] + C\left[s\theta(s) - \theta(0)\right] = 0$$

$$J\left[s^2\theta(s) - 0 - \omega_s\right] + C\left[s\theta(s) - 0\right] = 0$$

$$\theta(s) = \frac{\omega_s}{s\left(s + \frac{C}{J}\right)}$$

Taking partial Fraction,

$$\theta(s) = \omega_s \frac{J}{C}\left(\frac{1}{s} - \frac{1}{s + C/J}\right)$$

Taking inverse Laplace transform,

$$\theta(t) = \omega_s \frac{J}{C}\left(1 - e^{\frac{C}{J}t}\right)$$

Taking derivative,

$$\dot{\theta}(t) = \omega_s e^{-\frac{C}{J}t}$$

$$\ln\left(\dot{\theta}\right) = -\omega_s \frac{Ct}{J}$$

$$C = \frac{J\ln\left(\dot{\theta}\right)}{\omega_s t}$$

The procedure followed in order to derive value of C can be outlined as follows,

When the generator is running with a load (approximately 15%), the breaker is tripped. So that speed suddenly increases to a higher level above the synchronous speed and the main valve is gradually closed. Once the main valve is closed completely, the torque exerted by turbine becomes zero and due to viscous damping of the system, rotor speed starts to gradually decrease with time due to friction. Speed Vs time measurements are taken from the point of closing the main valve till the rotor speed is zero. Figure 3.8 shows the speed Vs time under viscous damping.

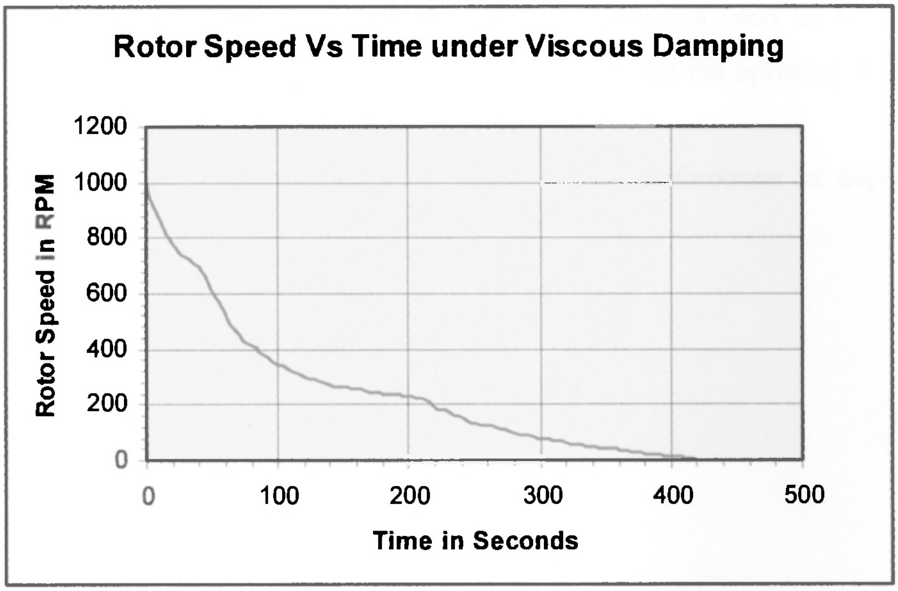

Figure 3.8 – Rotor Speed Vs Time when rotor spinning freely

Therefore, estimated value for C = 0.8 Kgm^2/sec

3.4.3 Estimation of P_m

Since the P_m deals with absolute power values around 1000 kW (at full load), it is required to find out an estimated values for P_m and K_T during the synchronization process. Synchronizer takes on its speed matching function when the rotor speed is ramped up to about 95% of the rated speed of the machine. In this scenario, experimentally measured time duration to effect 5% speed change is approximately 15 seconds.

Hence, Maximum value of P_m during synchronization is estimated as follows,

J = $250kgm^2$

Time Period = 15 sec

Speed change = from 712.5 RPM to 750 RPM

(from 74.613 rad/sec to 78.54 rad/sec)

$$P_m = \frac{250 * (78.54^2 - 74.613^2)}{15}$$

P_m = 10,024 W

3.4.4 Matlab Program to Estimate K, a & b

In order to estimate the PID values of the synchronizer, the present system's settling time is taken as the design parameter. The program used in Matlab is a computational method where program does the iterations till the optimum values are obtained.

The Matlab program used to find PID vales of the synchronizer is depicted in Appendix 1.

Results obtained from Matlab Program

Rise_time –

35

settling_time =

330

max_overshoot =

0.3475

Total system Transfer function:

$$\frac{\omega(s)}{\omega_s(s)} = \frac{1600\,s^2 + 453.3\,s + 18.66}{1.714e004\,s^4 + 6.29e004\,s^3 + 2.085e004\,s^2 + 514.2\,s + 18.66}$$

a = 0.2333, *b = 0.0500,* *K = 0.2000*

Transfer function of Synchronizer, governor and Turbine system:

$$\frac{1600\,s^2 + 453.3\,s + 18.66}{0.9\,s^3 + 3.3\,s^2 + s}$$

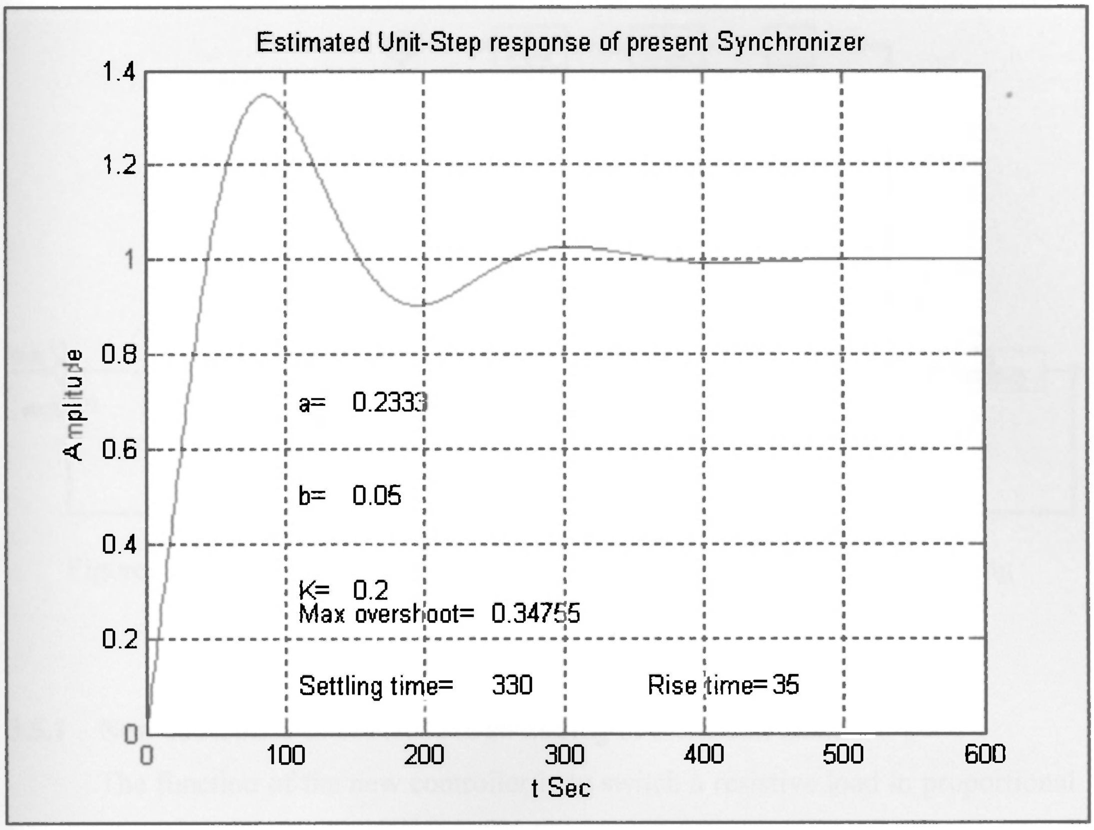

Figure 3.9 – Unit-Step response of present Mini-Hydro Generator.

3.5. Model of the Mini-Hydro Generator when 'Artificial Load' is connected during Synchronization.

During the synchronization process until the speed and phase angle are matched with the grid parameters and finally generator breaker is closed by synchronizer, $P_L(s)$ is zero. However, by introducing an Artificial load with a controlled PWM switching system an artificial resistive load $P_e(s)$ is applied to Generator during synchronization process. Then the power equilibrium of the hydro-turbine Generator will be as follows.

$$P_m(s) - P_e(s) = \omega_0(Js + C)\omega(s)$$

$$\omega(s) = \frac{P_m(s) - P_e(s)}{\omega_0(Js + C)}$$

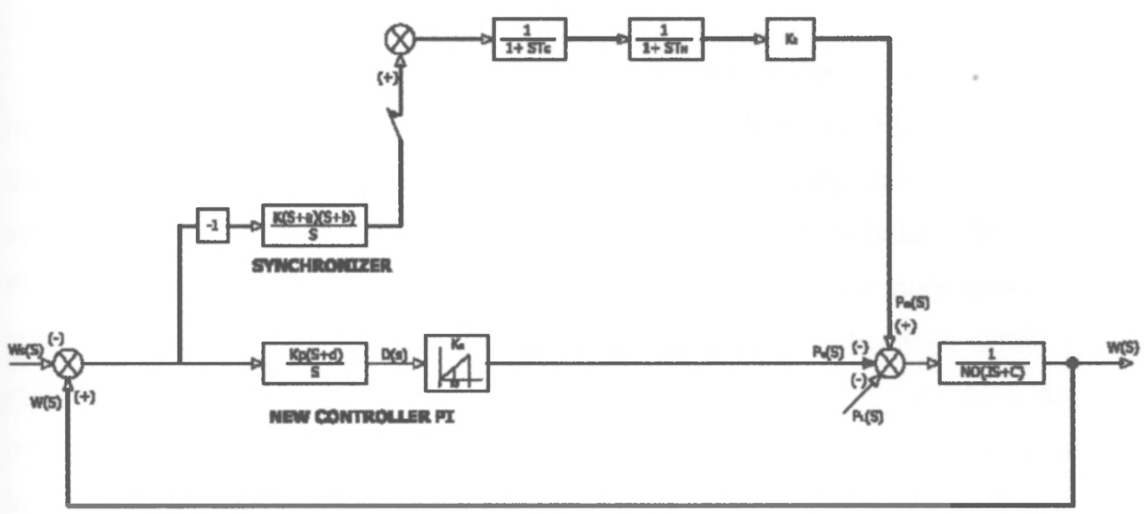

Figure 3.10 – Model of Mini-Hydro Generator with 'Artificial Load' during synchronization.

3.5.1 New controller to control the switching of Artificial Load

The function of the new controller is to switch a resistive load in proportional to actuating error e(s) (Proportional control) to incorporate damping to the system and thereby reduce the settling time. Moreover, it is required to settle the system exactly at reference input level of grid frequency, (Integrative Control) in order to support present synchronizer for rapid synchronizing. In this context, high sensitive speed error correction control action responding to rate of change of error (Derivative control) is not anticipated due to two main reasons,

1. Mini-Hydro generator synchronization is generally a slow process by the design itself because of the limitations pertaining to Prime mover system.
2. Derivative term could amplify disturbances input or noise as the PID is not well tuned. This can prompt oscillations or the system can become unstable. Further PID controller will permit fast changes of larger values of Artificial load, $P_e(s)$ to Generator which may disturb the Voltage matching process of AVR.

In the light of above considerations, a PI controller is more appropriate than a PID controller for switching the Artificial load, $P_e(s)$ for this application.

3.5.2 Matlab Program to Estimate K_P, d

Since a reasonable model of the present system is derived in 3.4.4, the modified system with Artificial load connected can be modeled. In order to estimate the PI values of the proposed new controller, the desired Settling time of the new system and Maximum overshoot are taken as design parameters. In order to find the PI values of the new controller a Matlab simulation techniques are more desirable over the experimental methods. The experimental results have to be taken within a minimum downtime of the plant. Therefore, for this particular project it is not practically viable to carry out fine tuning of PI parameters at site. The program used in Matlab to estimate PI parameters are detailed in Appendix 2.

Results obtained from Matlab Program

Rise_time =

5

settling_time =

42

max_overshoot =

0.0994

Transfer function:

$$\frac{\omega(s)}{\omega_s(s)} = \frac{4860\, s^4 + 1.969e004\, s^3 + 6851\, s^2 + 321.1\, s}{1.714e004\, s^5 + 6.776e004\, s^4 + 3.894e004\, s^3 + 6912\, s^2 + 321.1\, s}$$

Kp = 0.9000, *d = 0.0560,*

Transfer function of PI Controller:

$$\frac{0.9\, s + 0.0504}{s}$$

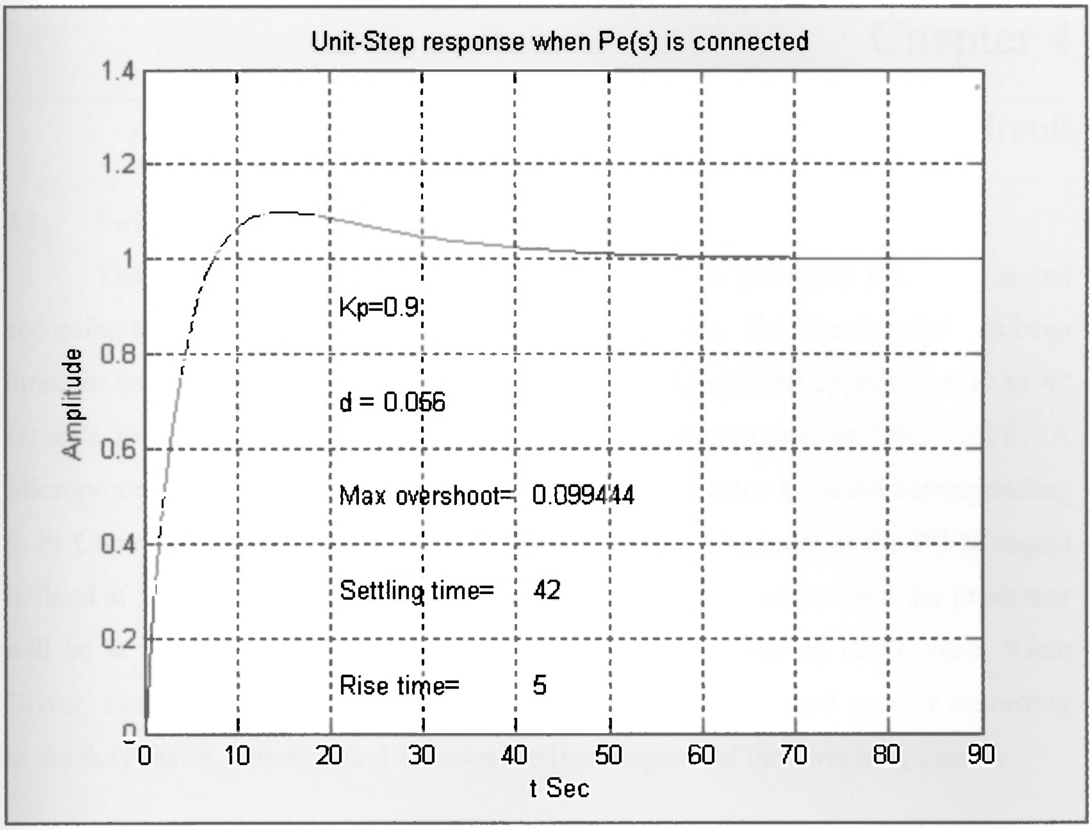

Figure 3.11 – Unit-Step response of the Mini-Hydro Generator when Artificial load is connected.

Chapter 4

Switching Circuit

4.1. Switching of Artificial load

The new PI controller as shown in Figure 3.10 generates a control signal according to the error e(s) during synchronization process. The PI controller has been tuned in such a way that the system 'Settling Time' is reduced approximately to 42 seconds following a step input. The PI controller programmed in 'PIC' 16F877A Microprocessor generates a PWM signal and the Duty Factor is varied corresponding to PI Controller's output control signal. The switching frequency of the PWM signal is fixed at 5 kHz in the processor. The magnitude of PWM pulses from the processor will be at 0-4.8 Volts which will be then given to the Gate of IGBT via a 'Gate Driver' circuit. Therefore, IGBT switches the load in a controlled manner according to the duty factor. The Figure 4.1 shows the line diagram of the switching circuit.

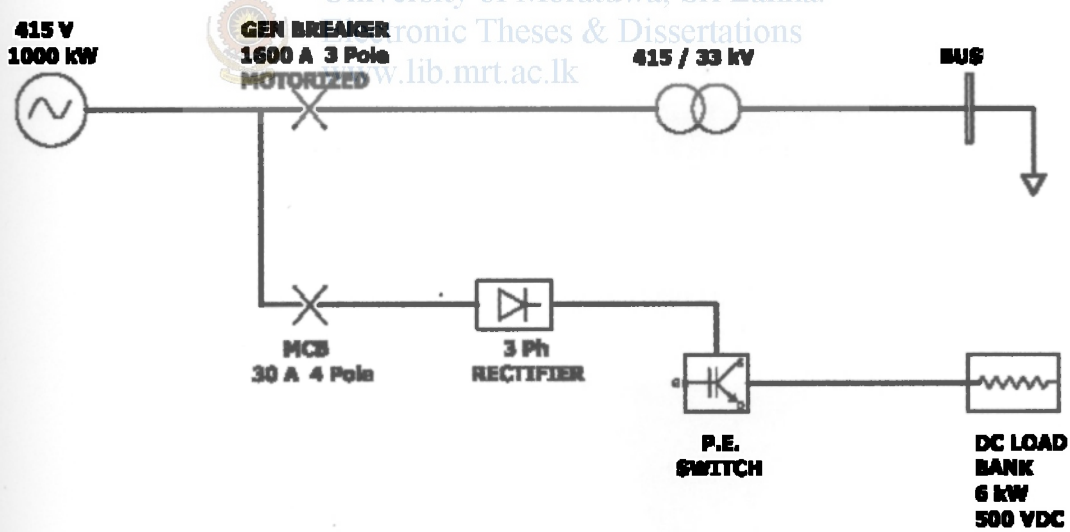

Figure 4.1 – Line Diagram of the Switching Circuit.

4.1.1 AC Power Supply from Generator Switchgear

The generator circuit breaker is used to connect and disconnect to and from the power system. As shown in the Figure 4.1, a 1600A, 3 Pole ACB type generator circuit breaker is located at the low voltage side of the step-up transformer (after Generator output terminals). The circuit breaker is closed as part of the generator synchronizing sequence and is opened or tripped either by operator control or by operation of any protective relay device in the event of unit fault condition.

For the new switching circuit, AC power supply connection is taken from the alternator terminals before the generator breaker and is then rectified through a three phase, six pulse rectifier circuit to convert AC to DC. The 3 phase supply at the alternator terminals are at 415 Volts and after full bridge rectification the DC Bus voltage will be around 560 Volts. The DC supply is then switched through the IGBT and power is consumed at the load bank as a resistive load.

4.1.2 The Resistive Load Bank

The capacity of the load bank is 5,812W which is built to operate at 560V DC supply. This comprises of four numbers resistive heater elements with a capacity of 1.5kW and 13.5Ω each. Since the heat dissipation from the elements is substantial the heater elements are cooled by a 3 phase induction motor driven blower fan of 0.37kW, 415V. The resistor configuration of the load bank is wired in series. Figure 4.2 shows the circuit of the Load Bank.

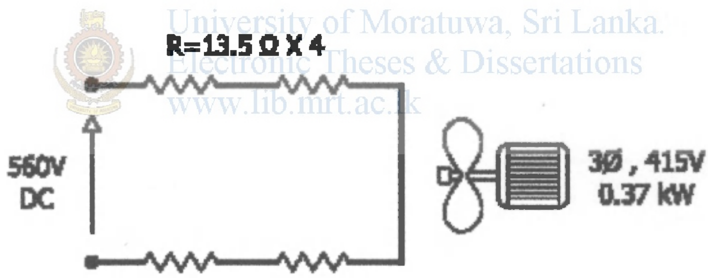

Figure 4.2 – Circuit of the DC Load Bank.

Figure 4.3 – A picture of the load bank, connected through a 30A/ 4P MCB

4.1.3 3 Phase Full Wave Diode Rectifier

Terminal AC Voltage to the rectifier	= 415 V
DC Bus Voltage	= 560.25 V DC
Maximum DC load current when the Duty Factor is 1.0	$= \dfrac{6000}{560.25}$ A
	= 10.375 A

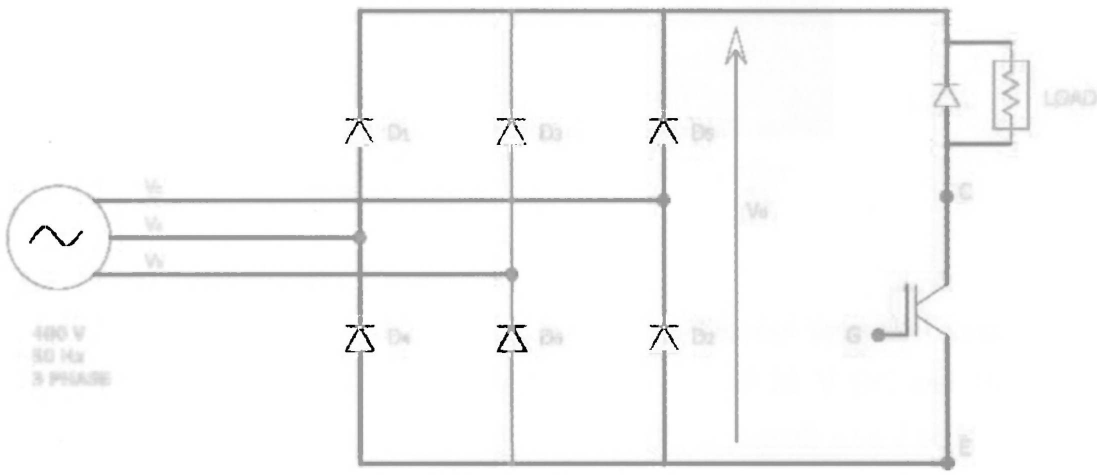

Figure 4.4 – 3 Phase Full Wave Diode Rectifier Circuit.

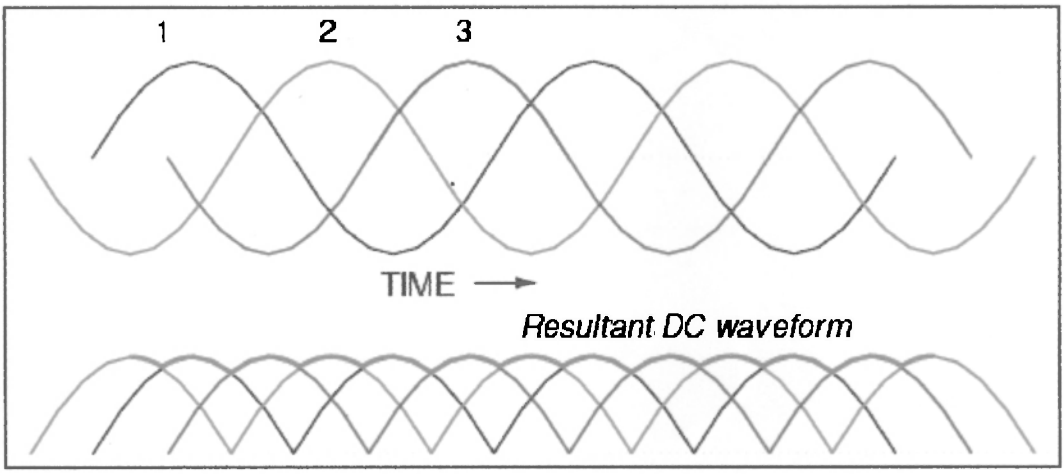

Figure 4.5 – DC waveform with Voltage Ripple after rectification (phase waveforms 1,2 and 3 are indicated in black, red and Blue colors respectively)

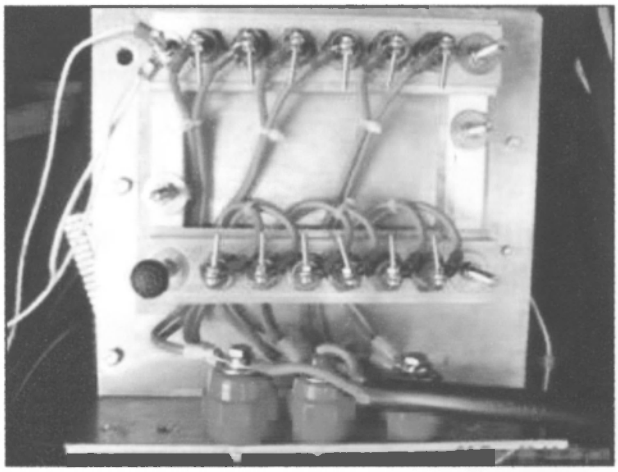

Figure 4.6 – A picture of 3 Phase Rectifier

4.1.4 IGBT Gate Driver Circuit

The maximum calculated Voltage and Current across the semi conductor switch in order to switch 6kW resistive load will be 560.25 V DC and 10.7 A respectively. The preset frequency of the switching (PWM signal) would be at 5 kHz which is within the limits of gate Driver switching transistor. Figure 4.7 shows a summery of device capabilities [6].

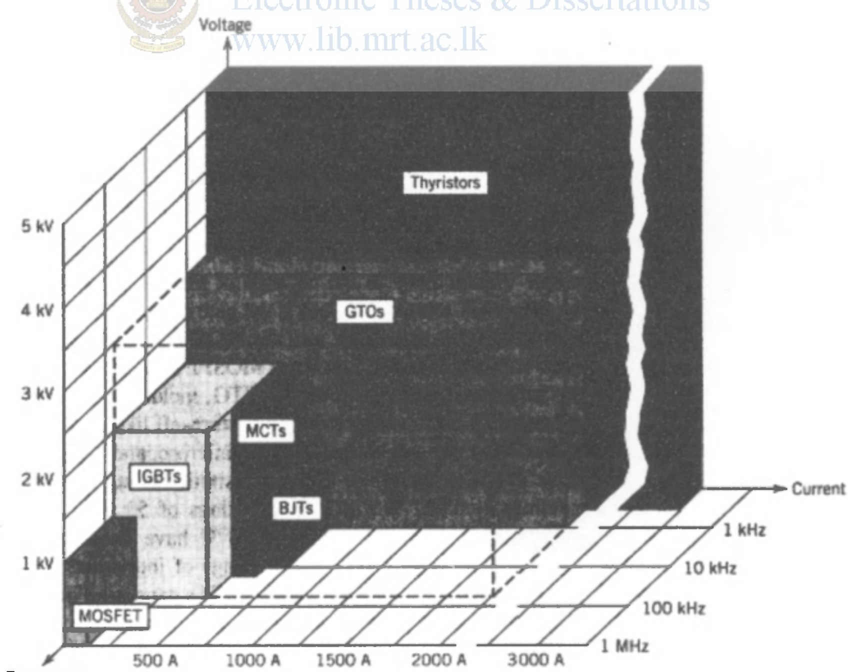

Figure 4.7 – Summery of semi conductor device capabilities. Source: Ned Mohan [6]

Therefore, based on the power capabilities, switching speed and considering the easiness of gate triggering by means of a voltage signal, an IGBT is selected as the switching device. Accordingly the selected IGBT model 'Toshiba-GT50J101' (Appendix 3) has the ratings of Collector-Emitter voltage of 600V and maximum Collector current of 50A.

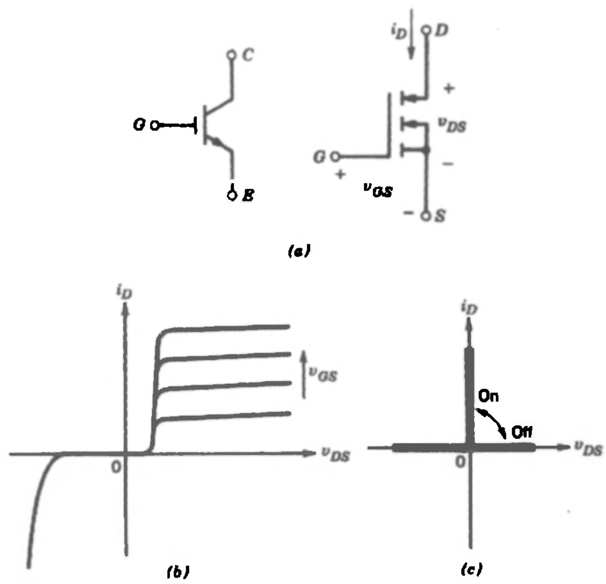

Figure 4.8 – An IGBT: (a) Symbol, (b) i-v characteristics (c) idealized characteristics.

Source: Ned Mohan [6]

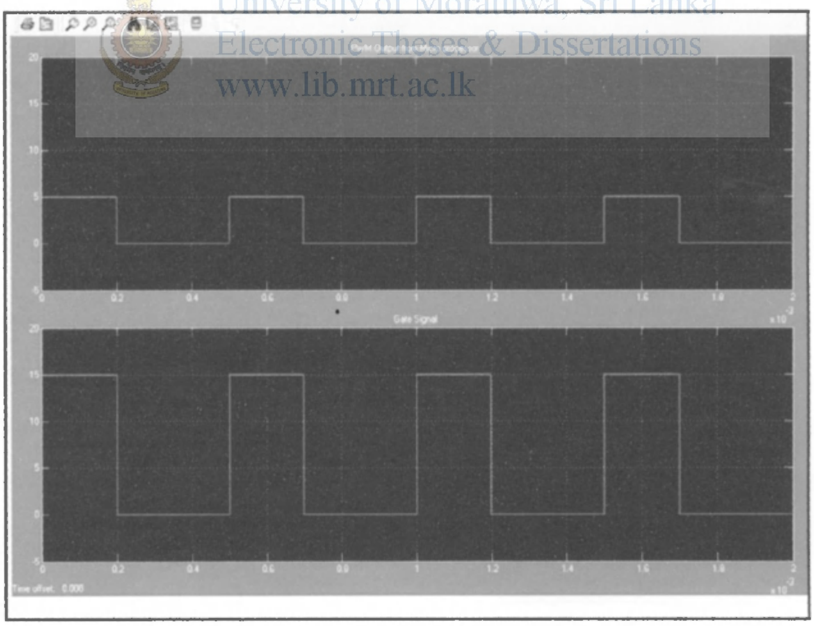

Figure 4.9 – PWM Output and Gate Signal to IGBT

In order to trigger the Gate, the PWM output signal from PIC16F877A (RC2, pin# 17) is isolated through the Optocoupler PC817 (Appendix 4) and connected to the gate at 15 Volts after amplification through a switching transistor. Figure 4.9 shows the details of the gate signal which is plotted at 40% Duty Factor and 5kHz switching frequency.

In order to amplify 0-4.8 V PWM signal to Gate driver signal at 0-15V a D313 (Appendix 5) switching Transistor is used. Figure 4.10 shows the details of the driver circuit.

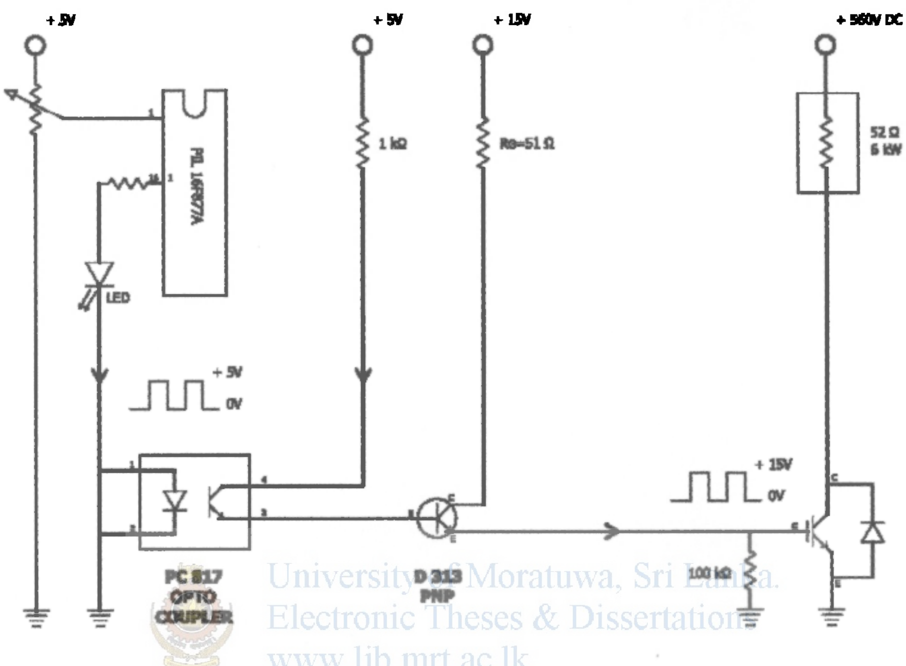

Figure 4.10 – IGBT Gate Driver Circuit

In order to provide DC power supplies for microprocessor, switching transistor triggering and IGBT gate driver separate 5V and 15V power supplies were used. AC step down transformer with full bridge rectification and smoothing capacitor was used for each DC supply. Since the output DC voltage levels have to be constant, LM7805 and LM7815 regulator ICs were used in 5V and 15V power supply circuits respectively.

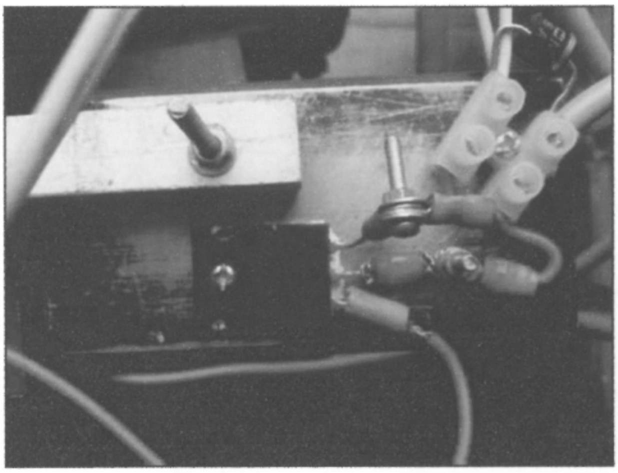

Figure 4.11 – A picture of the IGBT mounted on a Heat Sink.

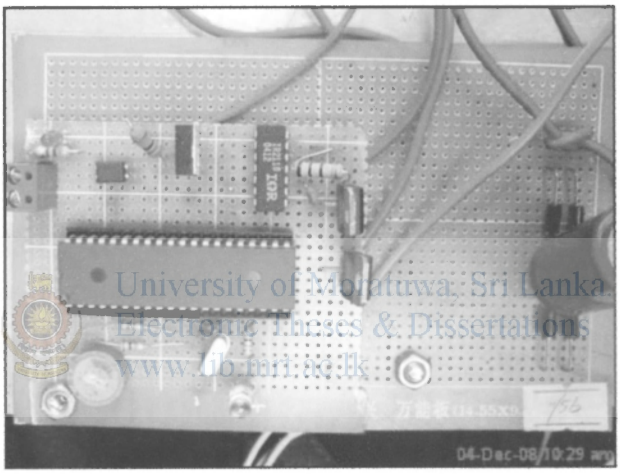

Figure 4.12 – A picture of PIC 16F877A Microprocessor based driver circuit.

4.1.5 Speed Sensing Circuit

In the model of the Mini-Hydro Generator when Artificial load is connected as shown in the Figure 3.10, it is required to sense the electrical speed of the grid supply as well as Generator supply at the summation point to generate speed error signal e(s). As denoted in the model ω_s and ω are the speed of grid supply and speed of generator supply respectively.

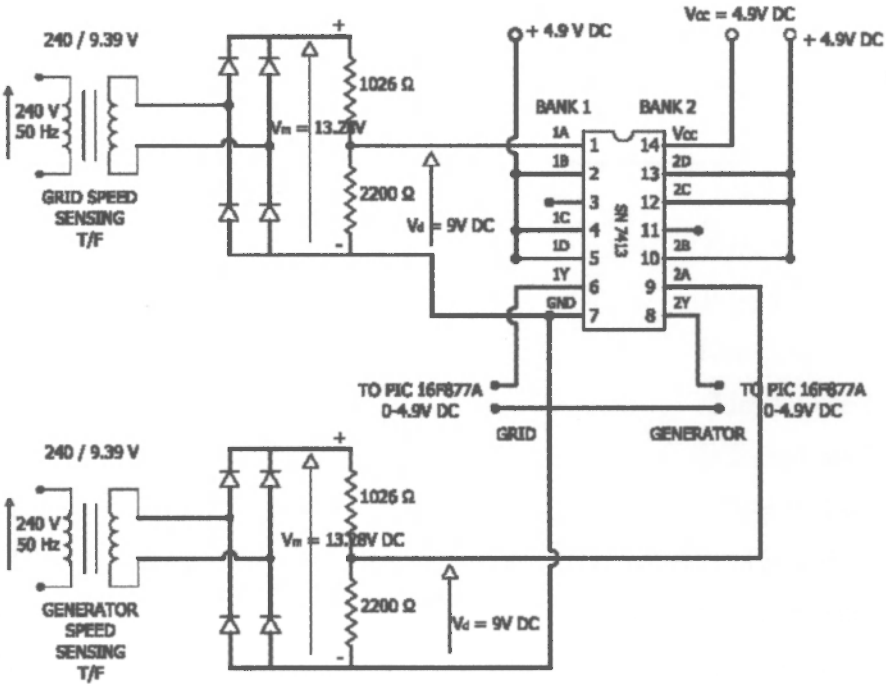

Figure 4.13 – Diagram of Speed Sensing Circuit.

As shown in Figure 4.13 two single phase step down transformers are used to sense the cycle speed of both sources. The two step down transformers used for this circuit are of 0-240V primary and 0-10 V, 1.8VA secondary output. Each is connected to the same phase (T_2 terminal) of both sources. The secondary 0-10V RMS output is rectified by a full bridge diode rectifier. The rectified signal voltage is then further reduced by a Voltage Divider before it is connected to the Schmitt Trigger SN7413. (Appendix 6)

Voltage at primary side of the transformer	= 240 V AC
Voltage at secondary side of the transformer	= 9.39 V AC
Maximum voltage (V_m) after full wave rectification	= 13.28 V DC
Voltage divider Resistor ratio (R_1 : R_2)	= 1046 Ω : 2200 Ω
Maximum voltage (V_m) after Voltage divider	= 9V DC

The above full wave rectified positive half Sine wave signal with 9 V DC Maximum Voltage is connected to Pin 1 (1A) of the Schmitt Trigger. At the Schmitt Trigger, high level reference voltage is preset at 4.9V DC at Pin 14. All other NAND gate pins 1B, 1C, 1D are given logic 1 (4.9V DC). Thus, full wave rectified signal at Pin1 is converted to Square wave pulses at Pin 6 (1Y). Table 4.1 shows the details of the Truth Table used for converting positive half cycle sine wave signal to square wave pulses.

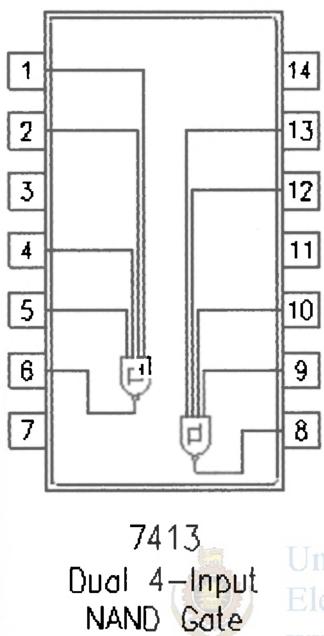

Pin Number	Description
1	A Input Gate 1
2	B Input Gate 1
3	Not Connected
4	C Input Gate 1
5	D Input Gate 1
6	Y Output Gate 1
7	Ground
8	Y Output Gate 2
9	A Input Gate 2
10	B Input Gate 2
11	Not Connected
12	C Input Gate 2
13	D Input Gate 2
14	Positive Supply

Figure 4.14 – Pin details of SN7413 Schmitt Trigger.

Table 4.1 - Truth Table of 4 input NAND gate with Hysteresis.

1A (pin 1) Full wave rectified sine wave input	1B(pin 2)	1C(pin 4)	1D(pin 5)	1Y(pin 6)	Reference (pin 14)	GND (pin 7)
> 4.9V⇒ 1	1	1	1	0	4.9V	0V
0.0V⇒ 0	1	1	1	1	4.9V	0V

Dual banks of the Schmitt Trigger are used to process the signals from Grid supply as well as Generator supply. The two such square wave signals derived from both sources are then connected at input pins RB6 and RB7 of Port B (pins 39 and 40) of the Microprocessor. The program in the microprocessor will check for the Phase Width of each square wave and then it is converted frequency. Then after comparing grid frequency against generator frequency, the difference will generate the error, denoted as e(s) in the model.

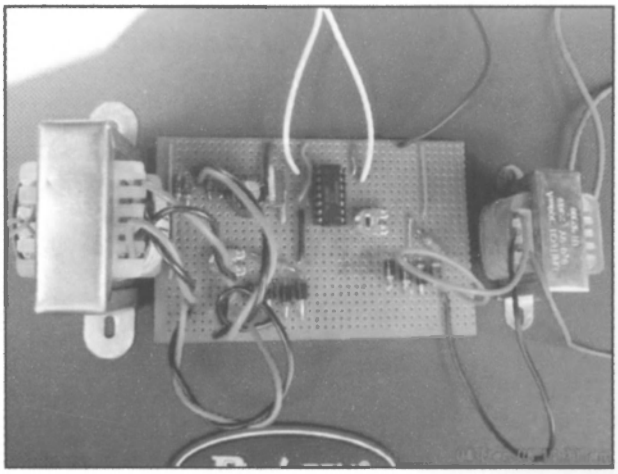

Figure 4.15 – A picture of Speed Sensing circuit

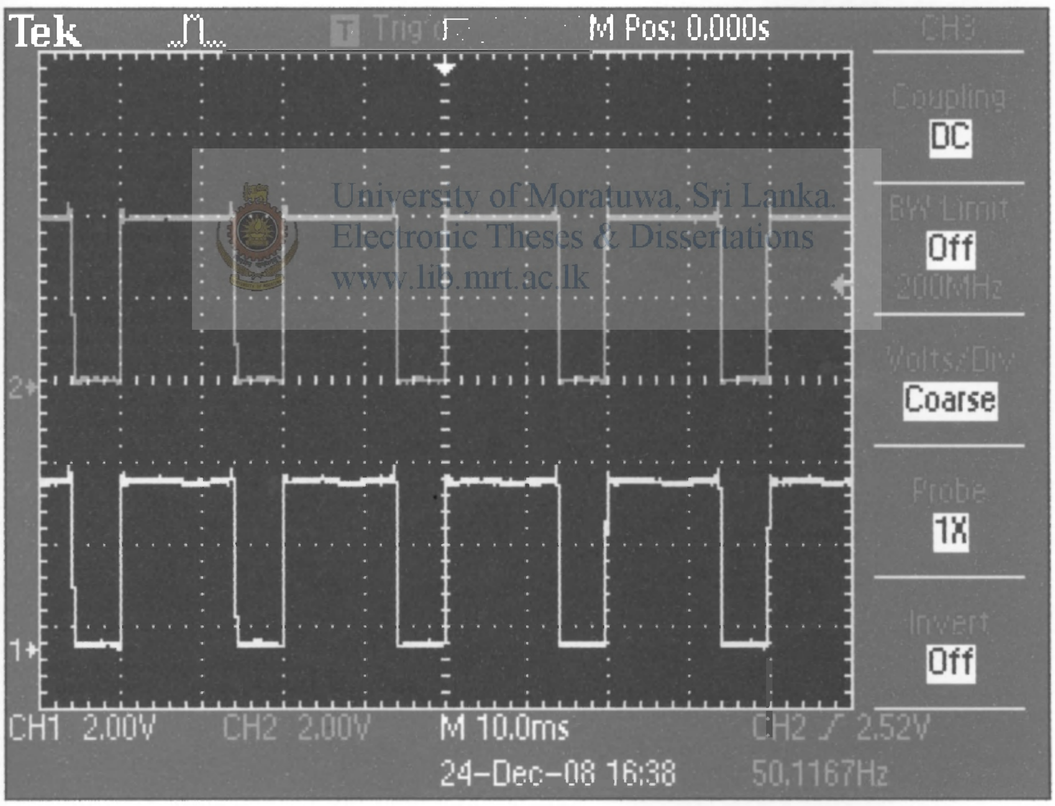

Figure 4.16 – Square wave signal output from Schmitt Trigger, converted from Sinusoidal voltage sources.

4.2. Installation of Prototype Circuit Module at site

At the beginning of the project, a desk survey was carried out to find out a suitable Mini-Hydro plant to experiment the prototype circuit module. Certain factors were considered during the survey such as plant capacity, easy accessibility, whether the plant is under warranty period and whether the plant's synchronization delay is significant factor. Having considered the above facts it was possible to decide on a 1MW plant 'Gomala-Oya' for practical implementation of the circuit module. After finalizing the project proposal, proposed circuit and its operation was discussed with the plant developer and permission was obtained to install and experiment this circuit module.

4.2.1 Termination of load Bank Power Cables

According to the site layout, the most appropriate location for tapping generator terminals for connecting power cables of Resistive Load bank is at the incoming side of the generator breaker at main Switchgear Panel. During a plant shutdown for maintenance, the termination of Load bank power cables were carried out. The end point of the power take off cable was terminated with a 30A, 3P MCB.

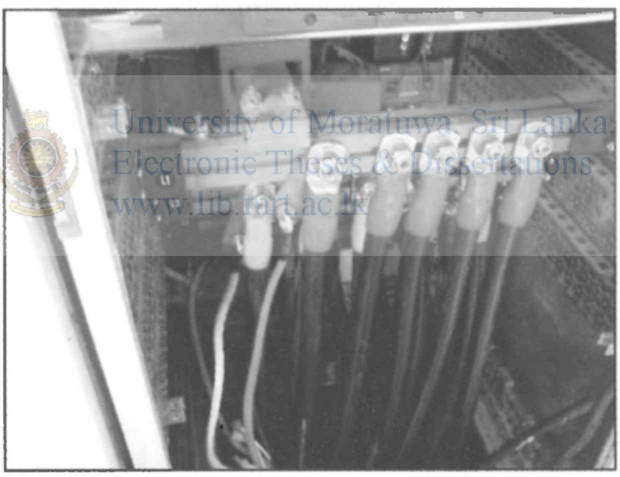

Figure 4.17 – A picture after connecting Load Bank cables at Generator terminals

Chapter 5

Switching Strategy

5.1. Introduction

In the present Mini-Hydro plant as the machine is started after a shutdown, the speed ramping is controlled by the PLC controller of the plant. As the speed of the rotor reaches 95% of the rated RPM, (712.5 RPM) the synchronizer takes over the synchronization process. In most of the times synchronizer can not synchronize the generator and close the breaker as the rotor speed reaches its rated speed. As depicted in Chapter 1, this synchronization process may take a few minutes depending on the plant design and control system.

In order to stabilize the rotor speed, a damping effect is introduced to the generator by switching a resistive load. The amount artificial load applied to the Generator during synchronization process is controlled by the new PI controller. The artificial load can be varied by the new PI controller in the range of 0-6kW by changing the duty factor. However, in the implementation of new controller, different switching strategies can be adopted in order to introduce the damping effect to the system.

5.1.1 Switching Strategy

Two alternative switching strategies can be implemented in order to achieve objective of damping the system. For the both alternative approaches PI controller parameters are the same and in broad terms the difference will be the initial value of the duty factor as the synchronization begins and variation of the duty factor during the synchronization period. They can be distinguished as follows,

I) Synchronization begins with Artificial Load ON state (0%< duty factor <50%)

II) Synchronization begins with Artificial Load OFF state (duty factor = 0%) and Load is switched (duty factor >0%) only when $\omega > \omega_s$

5.1.2 Strategy –(I) Synchronization begins with Artificial Load ON state (0% < duty factor <50%)

In this approach the Artificial Load is connected just prior to synchronization begins and as the synchronization starts, the duty factor already maintains a value between 30% to 50%. Accordingly, about 30-50% of the load (<3 kW) is already connected to the generator as the synchronization process is started. The load will stay connected with the system till the synchronization is completed and generator breaker is closed. The Figure 5.1 shows the model of this switching option.

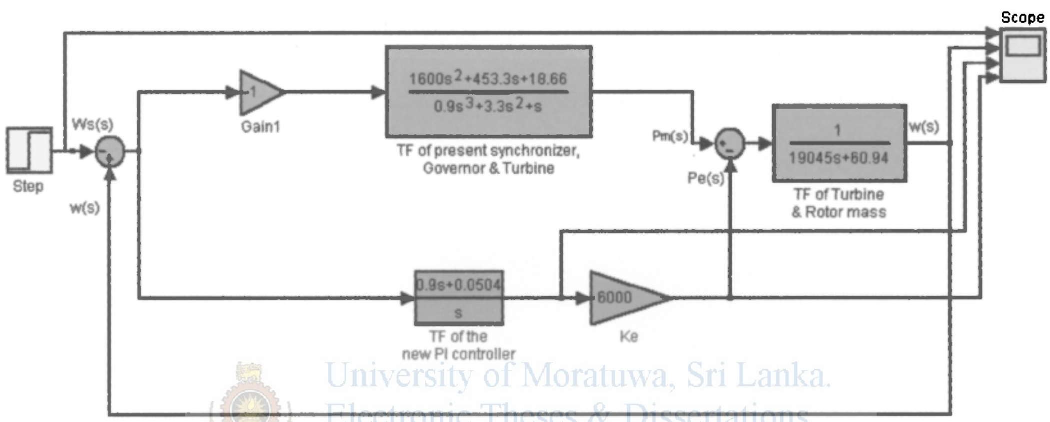

Figure 5.1 – Model of the system with Switching Strategy I.

The Duty Factor generated by microprocessor is exactly proportional to the PI control signal out put. In the above switching option simulation the PI control output signal variation is in the scale of -1 to +1 and Artificial load $P_e(s)$ variation is from 4000 to 0. However, the actual implementation in the circuit requires Duty Factor to be in the range of 0 to 1 and proportional $P_e(s)$ variation should be 0-6000 Watts. Physical interpretation of minus $P_e(s)$ refers to releasing of Artificial Load which had been loaded prior to synchronization begins. Accordingly, the program in PIC 16F877A is set such that Duty Factor is already reached to about 30-50% corresponding to 4000W (66.6% of $P_e(s)$) as the synchronization begins. The Figure 5.2 shows the results of the simulation.

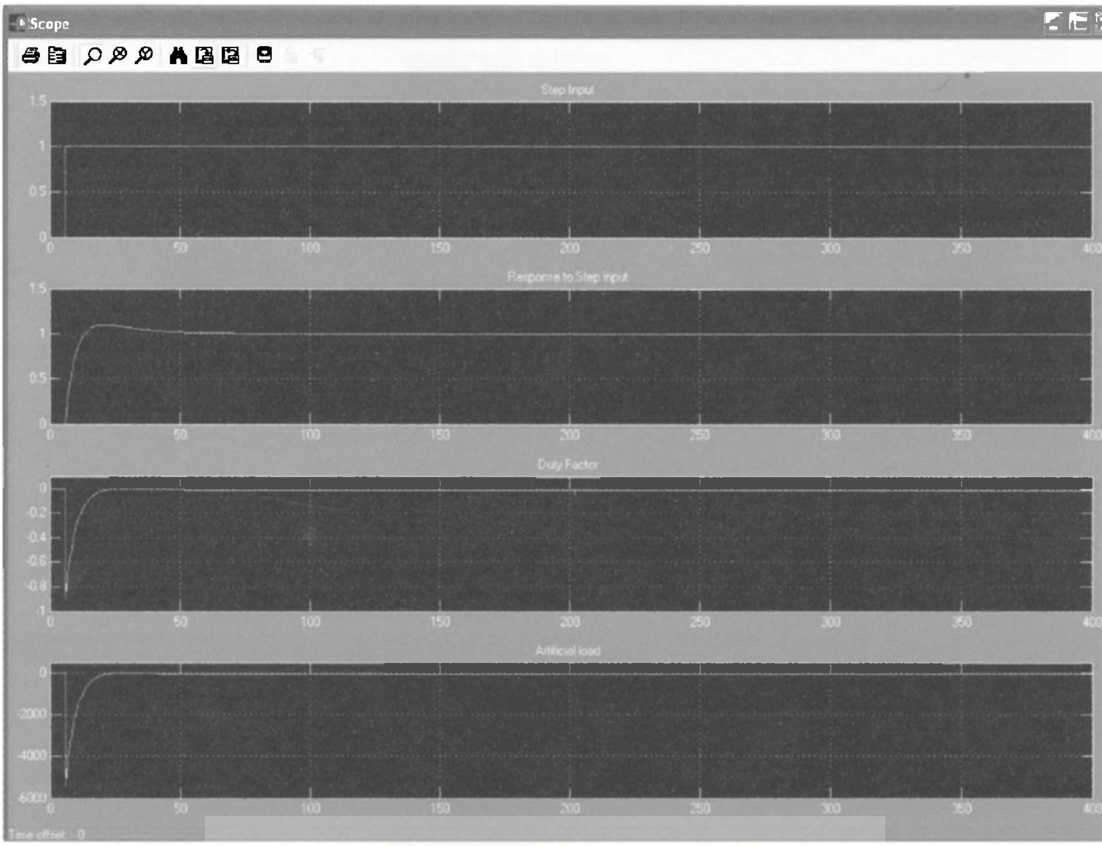

Figure 5.2 – Results of simulation with Switching strategy I.

5.1.3 Strategy –(II) Synchronization begins with Artificial Load OFF state (duty factor = 0%) and Load is switched (duty factor >0%) only when $\omega > \omega_s$

In this approach the Artificial Load is in its OFF state as the synchronization begins and therefore Duty Factor value is zero and accordingly $P_e(s)$ is also zero. As the rotor speed gradually increases to synchronize with the bus frequency and when it starts to go above the bus frequency, the PI controller provides the control signal output. Then corresponding Duty factor is generated by the processor and IGBT gate is switched according to the duty factor variation and finally $P_e(s)$ will be varied. Figure 5.3 shows the model of this switching option.

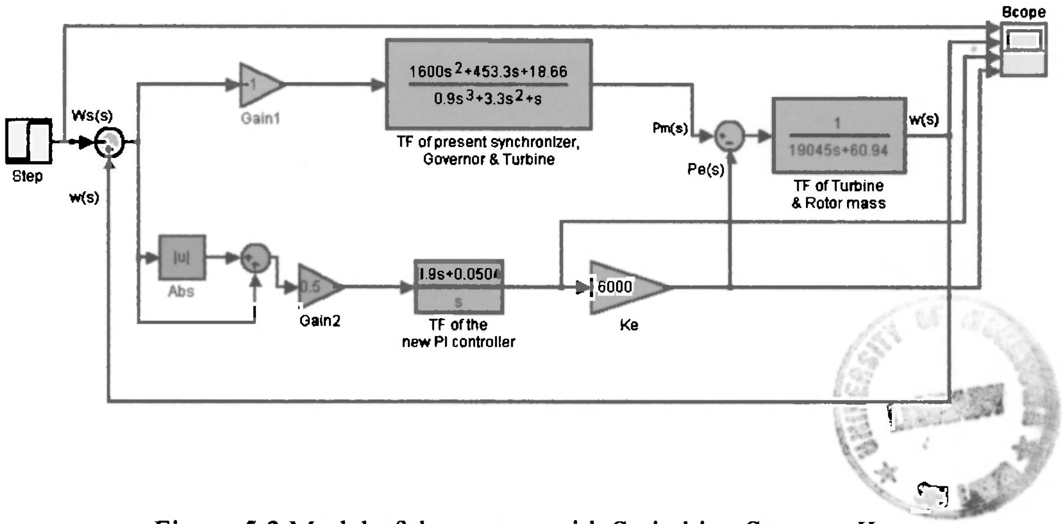

Figure 5.3 Model of the system with Switching Strategy II.

Figure 5.4 – Results of simulation with Switching strategy II.

According to the simulation of this switching option, the PI control out put signal variation is in the scale of 0 to 0.1. Therefore, microprocessor program will re-scale Duty Factor to be in 0-1 range and corresponding $P_e(s)$ will be 0- 6000 W range.

5.2. Observation of Simulation results

The observation of the simulation results in both cases can be summarized as in the Table 5.1 below.

Table 5.1 – Simulation of switching strategy I & II.

Performance Indices	Results of Present system	Results of New system			
		Strategy-I	Improvement	Strategy-II	Improvement
Rise time	**35 sec**	5 sec	**85.7%**	35 sec	**0%**
Settling time	**330 sec**	42 sec	**87.3%**	125 sec	**62.1%**
Max-Overshoot	**≏34.7%**	≏10%	**24.7%**	≏4%	**30.7%**
Duty Factor variation		1-0		0-0.6	
$P_e(s)$ variation		6-0kW		0-5kW	

Simulation results of individual switching strategy shows that both settling time and rise time are lower in the case of strategy I but it consumes the full capacity of the load bank initially and then reduced to zero. The maximum overshoot is comparatively higher than strategy II.

In contrast, Strategy II shows a low overshoot (4%). But the settling time is longer. However, both strategies show a significant performance over the present system.

The practical implementation of either of strategy can be achieved by changing the program in the PIC16F877A micro processor.

Chapter 6

Programming of Microprocessor

6.1. Continuous to Discrete conversion of PI Controller

The model of the present system has been derived in S plane by solving the differential equations in Laplace domain and accordingly proposed new PI controller for controlling the artificial load was derived as a continuous LTI model. The transfer function of PI controller developed in Matlab in S domain is as follows,

$$\textit{Continuous-time Transfer function of PI Controller} = \frac{0.9s + 0.0504}{s}$$

Since the design and implementation of the PI controller is performed in digital domain, it is discretized and converted to Z domain. In order to make the translation it is assumed that input is piecewise constant (zero-order hold). In this case, Sampling time T_s is taken as 0.04 seconds (40ms) which is determined by the time taken by CPU to detect a speed error between two digital pulse signals (from grid and generator sources). Conversion is made in Matlab using the commands listed below,


```
% tf of the new PI controller in S plane
Kp–0.9;
d–0.056;
num=[0 Kp Kp*d];
den=[0 1 0];
PI_TFc=tf(num,den)
PI_TFd=c2d(PI_TFc,0.04,'zoh')
```

Result: $\textit{Discrete-time Transfer function of PI Controller} = \frac{0.9z + 0.899}{z - 1}$

Sampling time: 0.04 sec

The above discrete PI controller is then simulated for both strategy I & II and corresponding responses to a step input are shown in Figure 6.2a and 6.2b respectively.

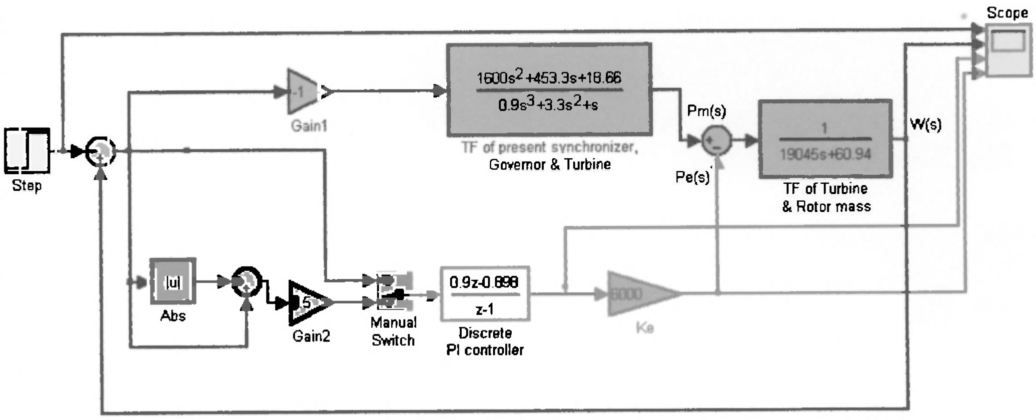

Figure 6.1 - Model of the system with discrete PI controller.

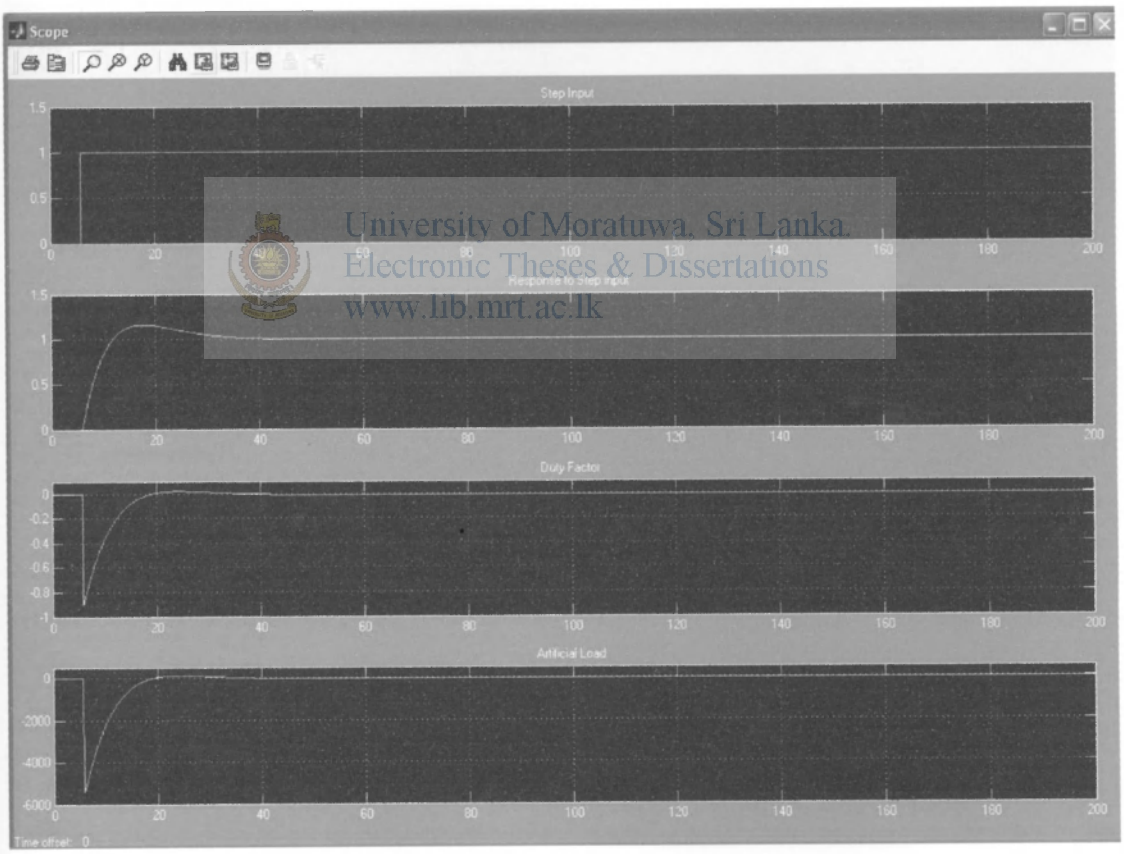

Figure 6.2a - Results of simulation with Switching strategy I, with discrete PI controller.

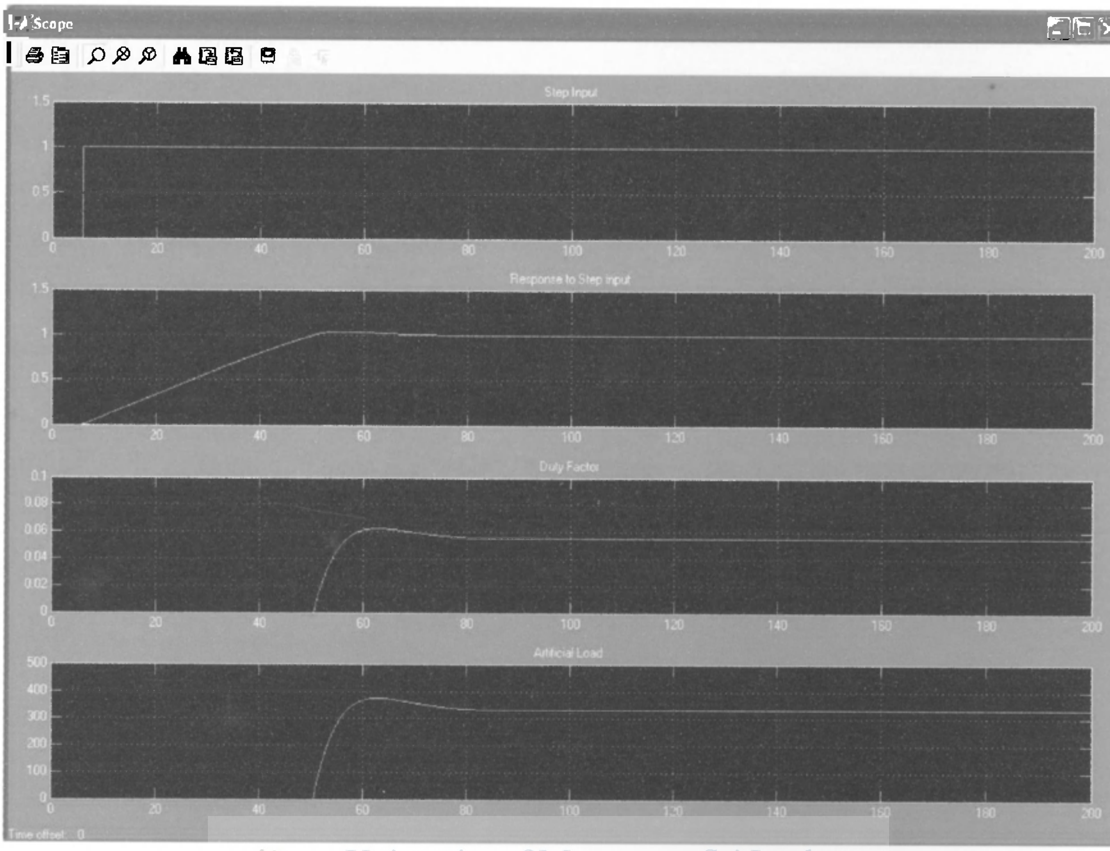

Figure 6.2b - Results of simulation with Switching strategy II, with discrete PI controller.

6.2. Comparison of simulation results for Continuous PI and Discrete PI controllers.

The response curves of the discrete PI controller obtained in Figure 6.2a and 6.2b exhibits small stair case shape in their response curves. However when compared with those of continuous PI controller responses in Figure 5.2 and 5.4. The both set of results are identical. Therefore, in the implementation of PI control algorithms in micro controller, the system is assumed to be continuous because the synchronization is a slow control system, and the sampling time 40msec is very small compared to settling time in the range of 40-150 seconds.

6.3. Selection of Microcontroller unit (MCU)

Currently, several manufacturers make 16-bit and 32-bit microcontrollers (MCUs) with features that enable easy control of almost any process of medium complexity. Eight-bit microcontrollers still dominate the market, however, because of their small size, low cost, and simple programming. Because of these advantages, 8-bit MCUs are found in process control, automotive, industrial, and appliance applications, among many others. Some of the newer MCUs provide clock speeds from 4 to 40MHz and 64KB of internal flash memory and 1KB of RAM in some models on-chip analog-to-digital converters (ADCs), digital-to-analog converters (DACs), or pulse-width modulator (PWM) outputs, a watchdog timer, 16-bits timers; and serial or USB ports.

In this section, the required CPU time to implement the proposed control strategies is estimated. There are mainly three parts in the time consumption for the CPU to achieve the switching strategy with PI controller,

(I) Speed Error sensing,

(II) PI Algorithm implementation,

(III) PWM output signal with Duty Factor variation proportional to PI control signal.

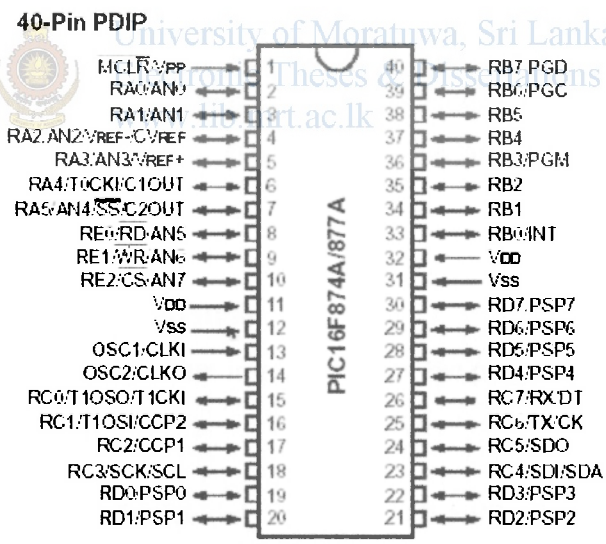

Fig 6.3 – Pin details of PIC16F877A microprocessor used for the PI controller.

6.3.1 Speed Error detection by Micro Processor

As shown in Figure 4.16, two square wave signals from grid and generator are fed in to Microprocessor input pins at R6 and R7 of Port B respectively. Methodology used in the Microprocessor program can be out lined as below.

Speed of the Crystal used in the PIC16F877A = 4MHz

Time Period per instruction = 1µsec

As the controller is switched ON the CPU first starts checking the bit status of pin R7 of Port B (grid source) continuously in a loop. If bit status is 0 (low), which means voltage level is 0 V, process will continue till bit status 1 (high) is commenced (positive edge detection). Then CPU starts counting the number of cycles till the bit status changes from 1 to 0 and again to 1 (next positive edge). This corresponds to a half cycle of grid frequency (10ms).

For counting the instruction cycles TIMER1 peripheral is used. And it has the capability of measuring the pulse widths up to 64ms. However, for our system we are interested around 10msec. If any pulse is longer than 65msec are neglected and the default output (0% PWM) is switched.

Then the process will shift to the generator source and will measure the phase width of the generator square wave. The plus or minus difference will generate the error. For the control purpose this error signal has to be converted to the frequency. In order to make the implementation less complicated a liner relationship is used and this relationship is accurate enough in the range that is interested in (50Hz to 54Hz). The error (in Hz) = error (in Sec) / 0.2, This algorithm deviates less than 4% in the range 50Hz to 54Hz.

6.3.2 PI Algorithm implementation

The continuous PI algorithm implemented in the program is as follows,

$$= \frac{0.9s + 0.0504}{s}$$

This algorithm is effective only when the, GENERATOR frequency > GRID frequency. In all other instances the PWM output will be set to default value which is 0% Duty. This increases settling time as previously discussed.

Then ,

The Proportional error term = Error (/Hz) * 0.9

The integral error term = sum (Error (/Hz)) * 0.504 / sampling time

sum (Error (/Hz)) is the cumulative error term

The resolution of the error frequency = 0.01Hz

To avoid steady state oscillation because of the integral term, an integral term limit function is implemented. Then the integral term will not increase after the integral error term value is reached to 10%, which will increase the steady state stability.

6.3.3 Generate Duty Factor of PWM in proportional to PI control signal.

The result of the PI controller was scaled to give the maximum output which is 100% duty factor at 4Hz error. The PWM frequency is selected to be in 5 KHz which is a fixed value. To generate this PWM signal the Capture Compare (CCP) module was used and the PWM output is connected to second pin at PORT C (RC2,CCP1, Pin# 17). In order ensure the smooth operation on a real-time system, resolution of the PWM is maintained at 0.4%

6.4. Programming of Microprocessor

Programming of the MCU is developed with assembly codes and key functions of the program such as generating error signal, PI algorithm, and PWM output are implemented. The compiler used for this project is Microchip MPLAB IDE V6.61.

The program is listed in Appendix 7, which is for switching strategy II after debugging it in the demonstration board and testing at workshop.

6.5. Outline to preliminary Testing of Circuitry.

The switching circuitry with PI controller was developed with the provision for experimenting both switching strategies as described in the previous chapters. Since, the testing of the circuitry and experimental results should be obtained within a minimum downtime of the plant at site, it was required to do a model testing of the circuitry in advance at workshop. Thus, to verify the PWM out put by PI controller according to speed error, a 24V DC motor was connected at the driver side (collector-Emitter) of IGBT. Using two signal generators, reference and feedback signals were simulated and thereby error signal was created. The resulting motor speed variation was observed and minor changes were done in the program.

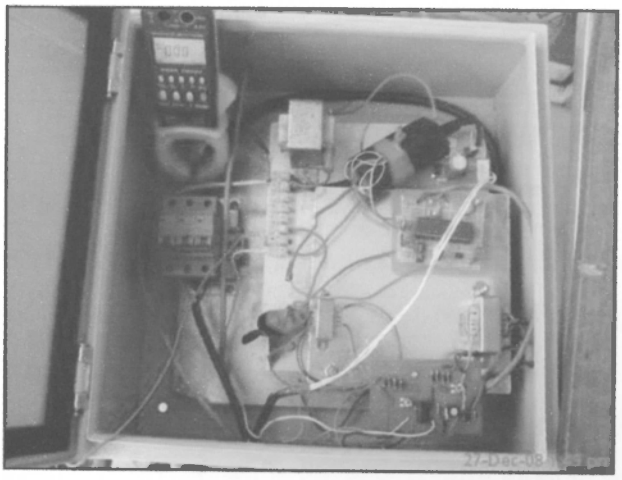

Fig 6.4 - A picture during testing, the complete controller circuit mounted inside an IP23 grade panel.

6.6. Installation of the sub-components of the circuit

The entire power and control circuitry complete with 3 phase diode bridge, Speed sensing circuit, PI controller with PWM unit and auxiliary DC power supply units (5V and 15V) were mounted in a IP23 class panel enclosure. The AC power input to the panel is connected to the 3 phase diode bridge through 30A, 3P MCB. The IGBT unit is mounted on a heat sink and it is installed near the cooling fan of the load bank to ensure proper heat dissipation from IGBT during switching.

Chapter 7

Experimental Results and Conclusion

7.1. Testing at Site

The new controller was temporally set up at site and a power analyzer model Fluke1735 was used to take the frequency Vs time readings during synchronization. For the speed sensing circuit, Voltage taping was taken from phase 2 of both sources (T_2 terminal). The testing was done for two switching methods. After setting up the new controller and power analyzer, while the new control module was in switched off state, the generator was given the starting signal and was allowed to synchronize as of normal operation. The frequency Vs time readings were recorded. The Figure 7.1 shows the synchronization under normal condition.

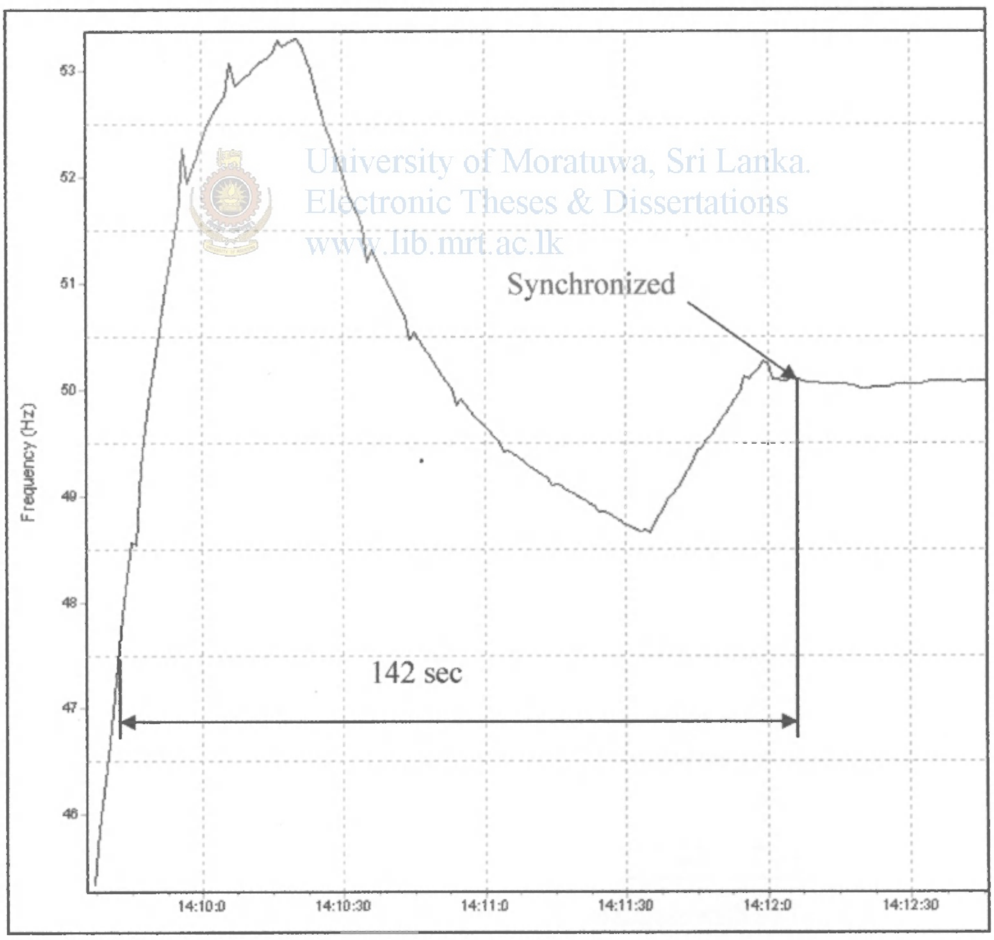

Figure 7.1 – Frequency Vs Time during synchronization under normal operation.

This is then taken as the reference to compare the differences or improvements happens when the system is subjected to artificial loading under switching strategy I & II. The synchronizing time 142 seconds indicated in Figure 7.1 is the time taken for synchronization.

7.2 Experimental Results with Switching Strategy I

After recording the measurements under normal synchronization, the generator was shutdown and the plant was restarted to take the results with the new controller enabled during synchronization. As per the simulation results given in the table 5.1, the MCU was programmed for switching strategy I (Take both +/- error) for the 1st testing. In this approach the Artificial Load was connected (with initial duty factor set to 40%) just prior to synchronization begins and as the synchronization starts, PI controller controlled the loading. The Figure 7.2 shows the synchronization under the strategy I.

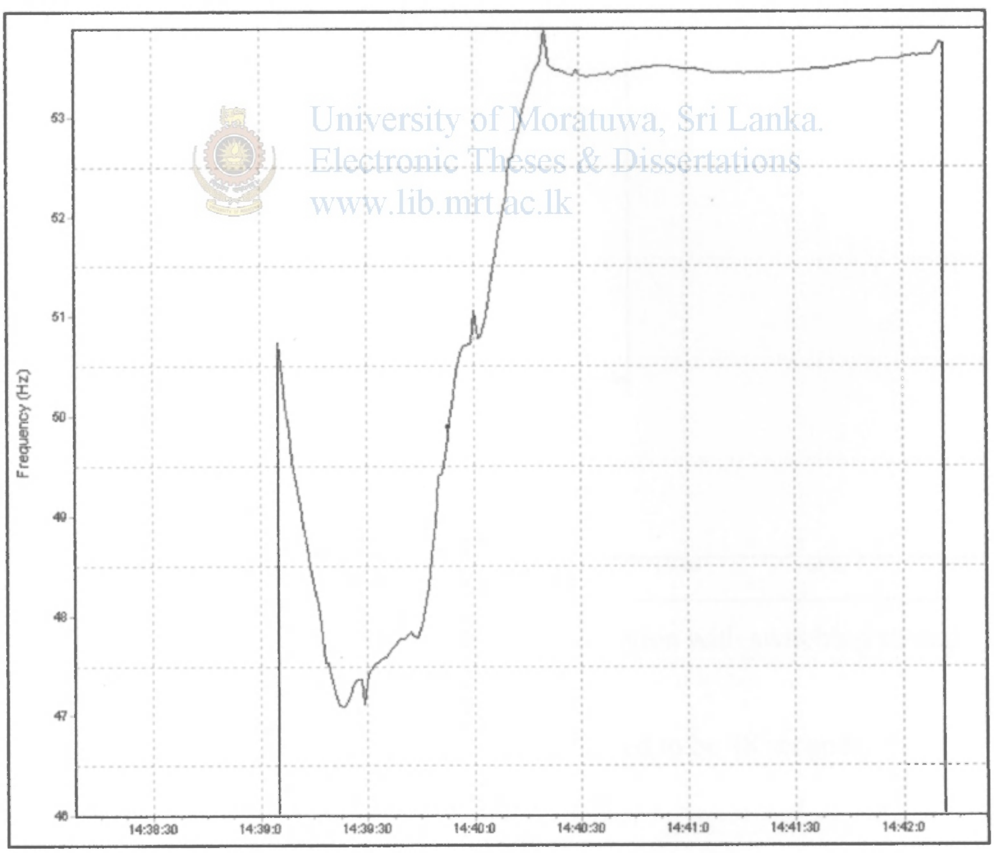

Figure 7.2 – Frequency Vs Time during synchronization with switching strategy I.

As per the resulting Frequency Vs Time curve in Figure 7.2, the frequency finally settles down at a much higher frequency (approximately 53.5 Hz equivalent to 802.5

RPM) where the synchronizing was not possible at that time and plant was shut down.

7.3 Experimental Results with Switching Strategy II

Under this method, the PI controller will respond only when error function (in Hz) is positive and when the error =0, duty factor=0, In that case, MCU signals a PWM output to the IGBT only when Generator frequency tries to exceed grid frequency. Thus the system operates as usual till to generator frequency tries to exceed 50Hz. The Figure 7.3 shows the frequency Vs time during synchronization when switching strategy II enabled.

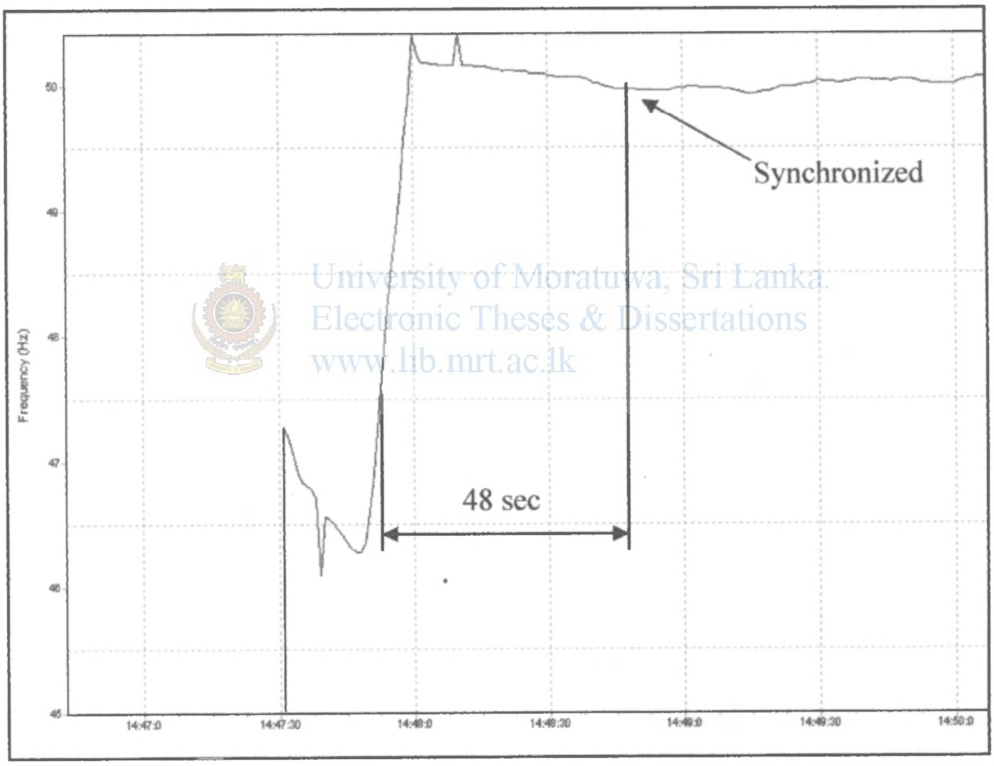

Figure 7.3 – Frequency Vs Time during synchronization with switching strategy II.

In this testing synchronizing time was measured to be 48 seconds.

7.4 Conclusion

The model of the present generator during synchronization was developed reasonably by taking known datasheet figures for generator, turbine and governor and taking estimated PID values for the synchronizer which were derived using a Matlab computational method. Thereafter, the PI values of the proposed new controller were estimated based on the above model. However, the real life response to switching strategy- I (Figure 7.2) has been deviated substantially compared to that of Matlab simulated results (Figure 5.2). In this approach the new controller is fully interacting with the control loop of present synchronizer, governor, turbine and generator loop as the synchronization begins. This will lead to involve both P_m and P_e at more or less equal power levels during ramping. Therefore, if the actual value of P_m subjects to a non linear behavior, the PI values of the new controller are no longer be valid. In such scenarios, more practical methods of tuning PI controller to be deployed. However, since the down time can not be permitted for prolonged testing purposes as it affects the energy production and revenue, such experimental methods for tuning PI values at site was not pursued.

In contrast, the results of the switching strategy II (Figure 7.3) are within the anticipated simulated results (Figure 5.4). In this option, the new controller starts to activate only when the generator frequency tries to exceed grid frequency. At this time the synchronizer signals negative pulses to reduce P_m and the synchronizer waits till the generator frequency slows down to reference frequency. Thus, during the positive loop of the generator frequency Vs time curve, the control loop combining PI controller-Generator dominates the speed control of the generator. Since the model maintains its linear characteristics the actual response is mostly in line with the simulated results.

When compared with the synchronization time between normal process and the synchronization with switching strategy II, the objective of the project has been achieved. The PI control action can be further fine tuned using trial and error methods at site when it comes to real commissioning. The time taken for synchronization has been reduced from 142 sec (Figure 7.1) to 48 sec (Figure 7.3). The maximum overshoot also has been reduced from 3.5Hz to 0.5Hz which is as a result of damping.

The time saving will save the downtime by 94 seconds and according to the Table 1.1 the plant can generate additional units of 376kWhrs per year assuming an average annual plant factor of 30%.

References

[1] Allen J. Wood and Bruce F. Wollenberg, *Power Generation Operation and Control*, 2nd ed., John Wiley & Sons, Singapore, 2005, Chapter 9, pp. 328-362.

[2] John J. Grainger and Willian D. Stevenson, Jr., *Power System Analysis*, McGraw-Hill, Inc., Singapore, 1994, Chapter 16, pp. 695-707.

[3] Katsuhiko Ogata, *Modern Control Engineering*, 4th ed., Prentice Hall of India Pvt. Ltd, New Delhi, 2006.

[4] Katsuhiko Ogata, *Discrete-Time Control Systems*, 2nd ed., Prentice Hall of India Pvt. Ltd, New Delhi, 2005.

[5] Cyril W. Lander, *Power Electronics*, 3rd ed., McGraw-Hill Book Co., Singapore, 1993.

[6] Ned Mohan, Tore M. Undeland and William P. Robbins, *Power Electronics*, 3rd ed., John Wiley & Sons Inc., Replika Press Pvt. Ltd., India, 2006 .

[7] James W. Dally, William F. Riley and Kenneth G. McConnell, *Instrumentation for Engineering Measurement*, 2nd ed., John Wiley & Sons Inc., Replika Press Pvt. Ltd., India, 2006, Chapter 6, pp. 162-205.

[8] Thomas C. Hayes and Paul Horowitz, *Student manual for The Art of Electronics*, Cambridge University Press, Gopsons Papers Limited, India, 2002. Chapter 2, pp. 82-140.

[9] Website, http://www.allaboutcircuits.com/vol2/chpt12/6.html, accessed on 4/06/2008.

[10] Data sheet # DS39582B *for PIC16F87XA 28/40 pin 8-bit CMOS flash, Microcontrollers,* Microchip Technology Inc., U.S.A, 2003.

[11] Data sheet # GT50J101 for 600V, 50A IGBT, Toshiba, Japan.

[12] Data sheet # PC817, Photocoupler, Sharp, Japan.

[13] Datasheet # UTC D313, NPN Switching Transistor, Unisonic Technologies Co., Ltd.

Appendix 1.

The Matlab program used to find PID vales of the present synchronizer

```
% Estimate PID values of present synchronizer, [K(s+a)*(s+b)/s]
J=250;
Wo=76.18;
C=0.8;
t=0:1:600;
Tg=0.3;
Th=3.0;
a=0.2333;
Kt=8000;
for K=0.2:-0.01:0.01; %starts the inner loop to vary the a values
for b=0.6:-0.001:0.001; %starts the inner loop to vary the a values
num1=[K (a+b)*K a*b*K];
den1=[0 1 0];
tf1=tf(num1,den1);
num2=[0 0 1];
den2=[0 Tg 1];
tf2=tf(num2,den2);
num3=[0 0 1];
den3=[0 Th 1];
tf3=tf(num3,den3);
num4=[0 0 1];
den4=[0 Wo*J Wo*C];
tf4=tf(num4,den4);
tf5=tf1*tf2*tf3*tf4*Kt;
sys=feedback(tf5,1);
y=step(sys,t);
m=max(y);
n=min(y);
if m<1.35 & m>0.99;
break; % breaks the inner loop
end
end
if m<1.35 & m>0.99;
```

```
break; % breaks the inner loop
end
end
r1=1;while y(r1)<0.1,r1=r1+1;end;
r2=1;while y(r2)<0.9,r2=r2+1;end;
Rise_time=(r2-r1)*1
s=601; while y(s)>0.98 & y(s)<1.02; s=s-1;end;
settling_time=(s-1)*1
max_overshoot=m-1
plot(t,y);
grid;
title('Estimated Unit-Step response of present Synchronizer')
xlabel('t Sec')
ylabel('Amplitude')
aa=num2str(a); %string value of 'a' to be printed on the plot
bb=num2str(b); %string value of 'b' to be printed on the plot
kk=num2str(K); %string value of 'K' to be printed on the plot
mm=num2str(max_overshoot); %string value of max_overshoot to be printed on the plot
rr=num2str(Rise_time); %string value of Rise_time to be printed on the plot
ss=num2str(settling_time); %string value of settling_time to be printed on the plot
text(110,0.7,'a='),text(150,0.7,aa)
text(110,0.5,'b='),text(150,0.5,bb)
text(110,0.3,'K='),text(150,0.3,kk)
text(110,0.25,'Max overshoot='),text(250,0.25,mm)
text(360,0.1,'Rise time='),text(450,0.1,rr)
text(110,0.1,'Settling time='),text(250,0.1,ss)
sol=[sys]
sol=[K;b]
TF_of_Present=tf1*tf2*tf3*Kt
```

Appendix 2.

The program used in Matlab to estimate PI parameters

```
% Estimate parameters for new PI controller when Pe(s) is connected, [K(s+d)/s]
J=250;
Wo=76.18;
C=0.8;
t=0:1:90;
Tg=0.3;
Th=3;
K=0.2;
a=0.2333;
b=0.05;
Kt=8000;
Ke=6000;
for Kp=0.9:-0.1:0.1; %starts the inner loop to vary the 'Kp' values
for d=0.1:-0.001:0.001; %starts the outer loop to vary the 'd' values
num1=[K (a+b)*K a*b*K];
den1=[0 1 0];
tf1=tf(num1,den1);
num2=[0 0 1];
den2=[0 Tg 1];
tf2=tf(num2,den2);
num3=[0 0 1];
den3=[0 Th 1];
tf3=tf(num3,den3);
tf4=tf1*tf2*tf3*Kt;
%tf of the new PI controller
num4=[0 Kp Kp*d];
den4=[0 1 0];
tf5=tf(num4,den4);
tf6=tf5*Ke;
Gc=parallel(tf4,tf6);
num5=[0 0 1];
den5=[0 Wo*J Wo*C];
Gp=tf(num5,den5);
```

```
sys=feedback(Gc*Gp,1);
y=step(sys,t);
m=max(y);
if m<1.1 & m>0.99;
break; % breaks the inner loop
end
end
if m<1.1 & m>0.99;
break; % breaks the inner loop
end
end
r1=1;while y(r1)<0.1,r1=r1+1;end;
r2=1;while y(r2)<0.9,r2=r2+1;end;
Rise_time=(r2-r1)*1
s=91; while y(s)>0.98 & y(s)<1.02; s=s-1;end;
Settling_time=(s-1)*1
max_overshoot=m-1
plot(t,y);
grid;
title('Unit-Step response when Pe(s) is connected')
xlabel('t Sec')
ylabel('Amplitude')
kk=num2str(Kp); %string value of Kp to be printed on the plot
dd=num2str(d); %string value of d to be printed on the plot
mm=num2str(max_overshoot); %string value of max_overshoot to be printed on the plot
ss=num2str(Settling_time); %string value of Settling_time to be printed on the plot
rr=num2str(Rise_time); %string value of Rise_time to be printed on the plot
text(21,0.9,'Kp='),text(26,0.9,kk)
text(21,0.7,'d ='),text(26,0.7,dd)
text(21,0.5,'Max overshoot='),text(42,0.5,mm)
text(21,0.3,'Settling time='),text(42,0.3,ss)
text(21,0.1,'Rise time='),text(42,0.1,rr)
sol=[sys]
sol=[Kp;d]
Kp=Kp
d=d
tf4
```

```
TF_of_PI=tf(num4,den4)
PIc2d=c2d(tf5,0.04,'zoh')
```

Appendix 3

737-914

GT50J101

IGH POWER SWITCHING APPLICATIONS.

- High Input Impedance
- High Speed : t_f=0.35μs(Max.)
- Low Saturation Voltage : $V_{CE(sat)}$=4.0V(Max.)
- Enhancement-Mode

Unit in mm

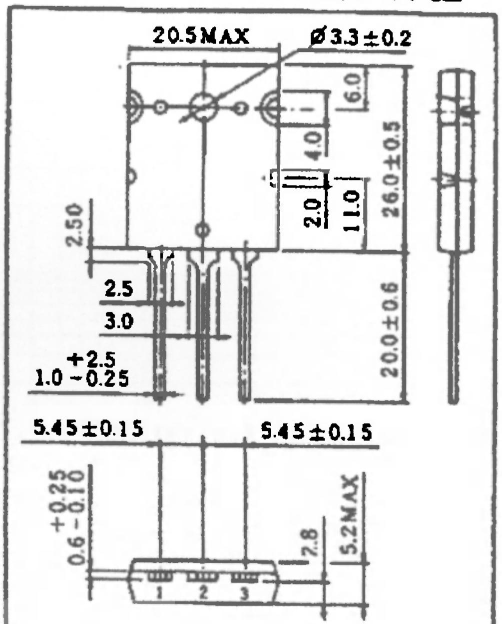

1. GATE
2. COLLECTOR (HEAT SINK)
3. EMITTER

JEDEC	—
EIAJ	—
TOSHIBA	2-21F1C

Weight : 9.75g

AXIMUM RATINGS (Ta=25°C)

CHARACTERISTIC		SYMBOL	RATING	UNIT
ollector-Emitter Voltage		V_{CES}	600	V
ate-Emitter Voltage		V_{GES}	±20	V
ollector Current	DC	I_C	50	A
	1ms	I_{CP}	100	
ollector Power Dissipation (Tc=25°C)		P_C	200	W
unction Temperature		T_j	150	°C
torage Temperature Range		T_{stg}	-55~150	°C
crew Torque		-	0.8	Nm

LECTRICAL CHARACTERISTICS (Ta=25°C)

CHARACTERISTIC		SYMBOL	TEST CONDITION	MIN.	TYP.	MAX.	UNIT
ate Leakage Current		I_{GES}	V_{GE}=±20V, V_{CE}=0	-	-	±500	nA
ollector Cut-off Current		I_{CES}	V_{CE}=600V, V_{GE}=0	-	-	1.0	mA
ollector-Emitter reakdown Voltage		$V_{(BR)CES}$	I_C=2mA, V_{GE}=0	600	-	-	V
ate-Emitter Cut-off Voltage		$V_{GE(off)}$	I_C=50mA, V_{CE}=5V	3.0	-	6.0	V
ollector-Emitter aturation Voltage		$V_{CE(sat)}$	I_C=50A, V_{GE}=15V	-	3.0	4.0	V
nput Capacitance		C_{ies}	V_{CE}=10V, V_{GE}=0, f=1MHz	-	3500	-	pF
witching Time	Rise Time	t_r	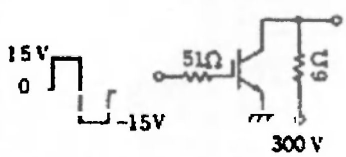	-	0.3	0.6	μs
	Turn-on Time	t_{on}		-	0.4	0.8	
	Fall Time	t_f		-	0.15	0.35	
	Turn-off Time	t_{off}		-	0.50	1.00	
hermal Resistance		$R_{th(j-c)}$	-	-	-	0.625	°C/W

SWITCHING TIME — I_C

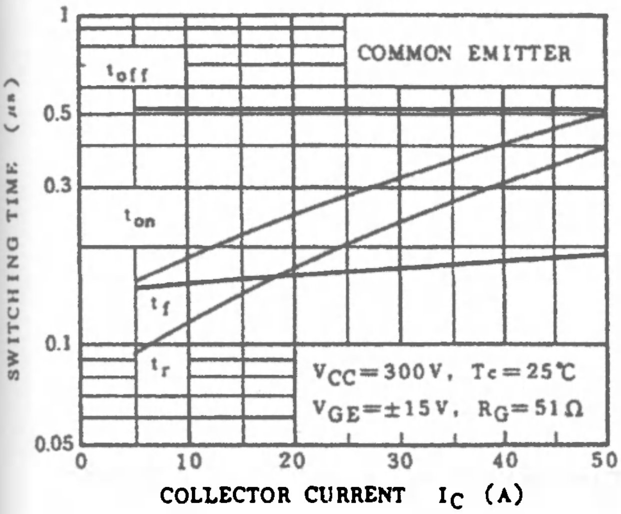

SWITCHING TIME — R_G

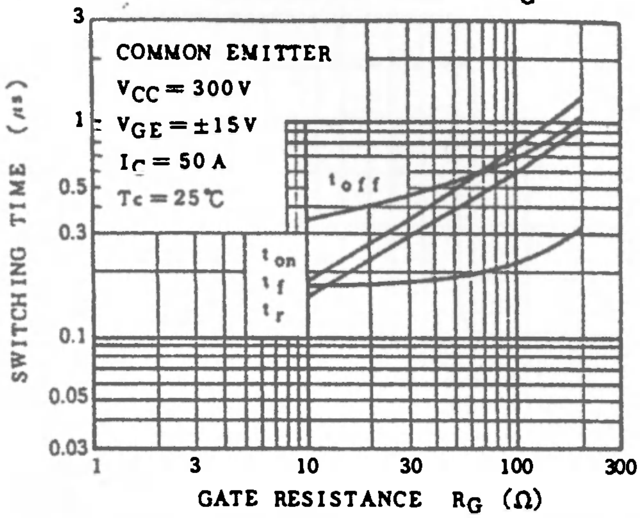

C — V_{CE}

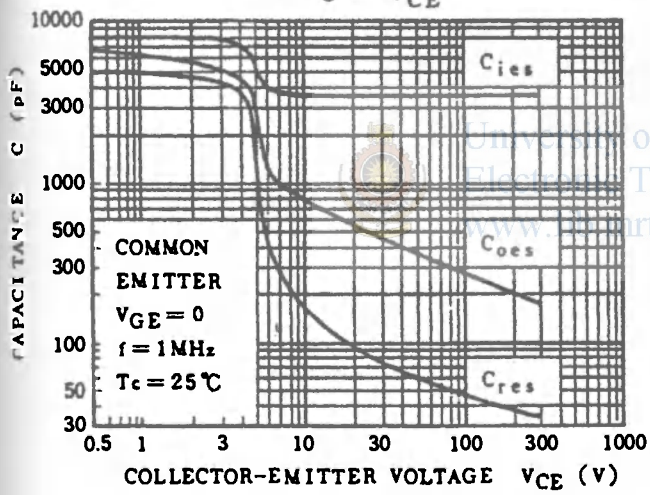

$R_{th(t)}$ — t_w

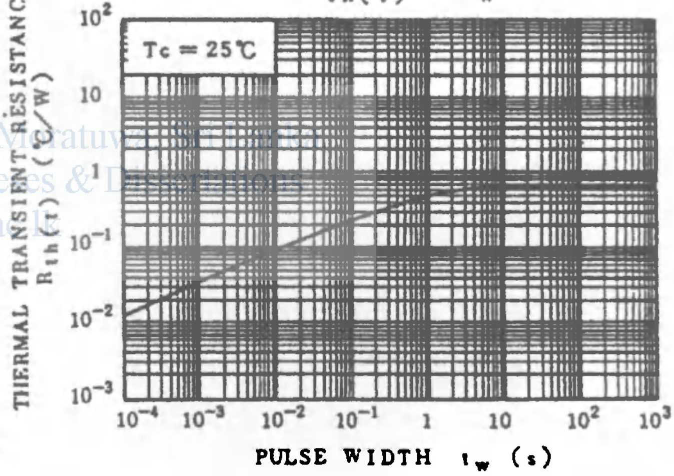

SAFE OPERATING AREA

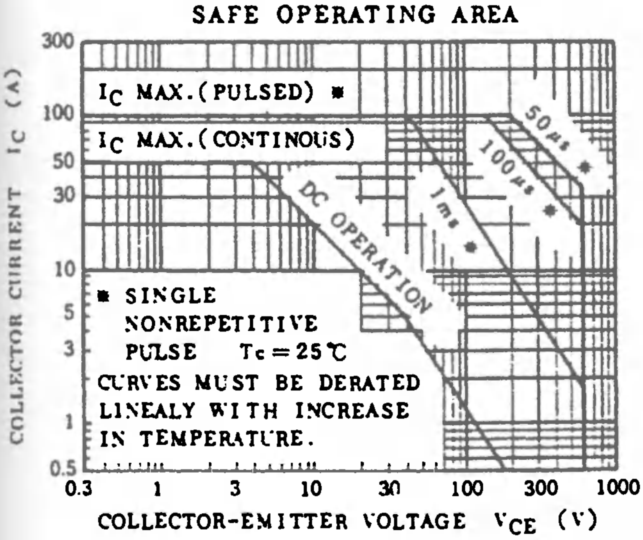

REVERSE BIAS SOA

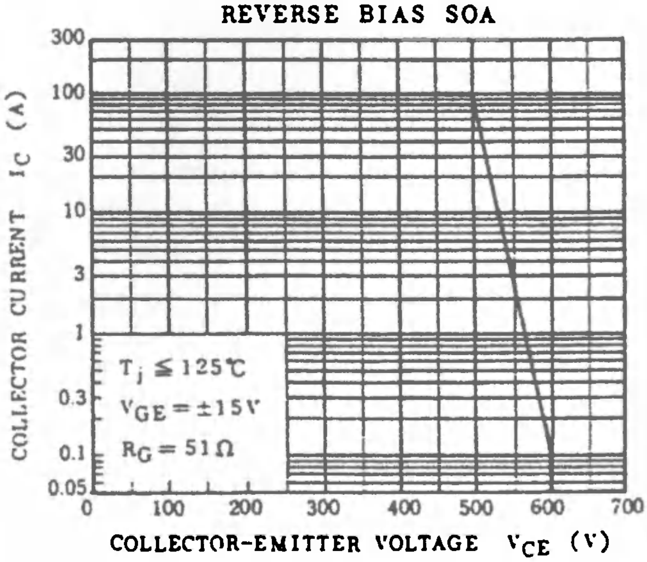

$I_C - V_{CE}$

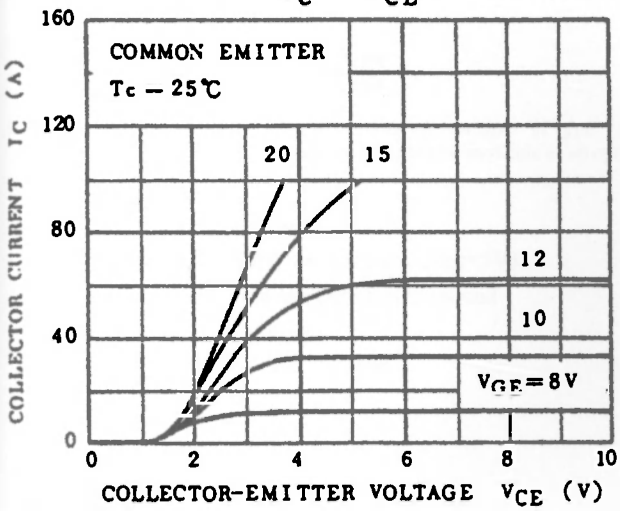

$V_{CE} - V_{GE}$

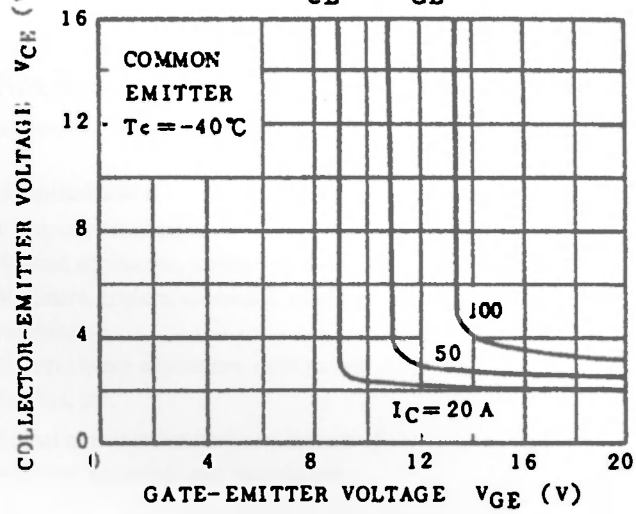

$V_{CE} - V_{GE}$

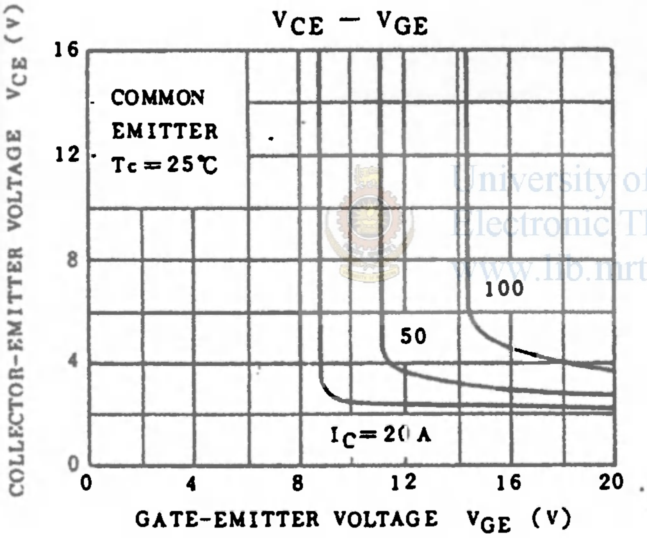

$V_{CE} - V_{GE}$

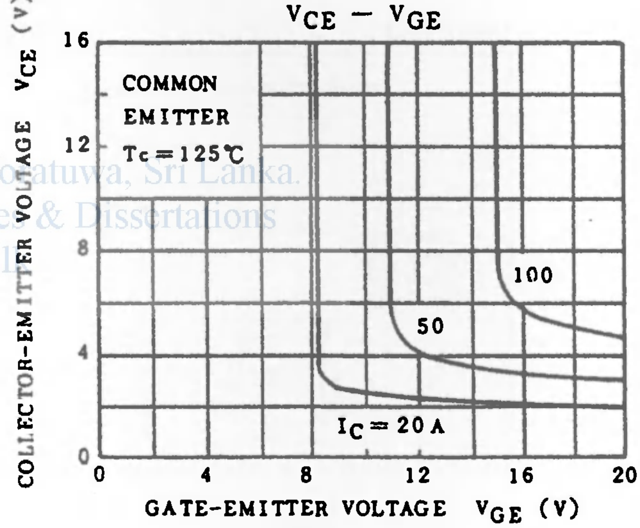

$I_C - V_{GE}$

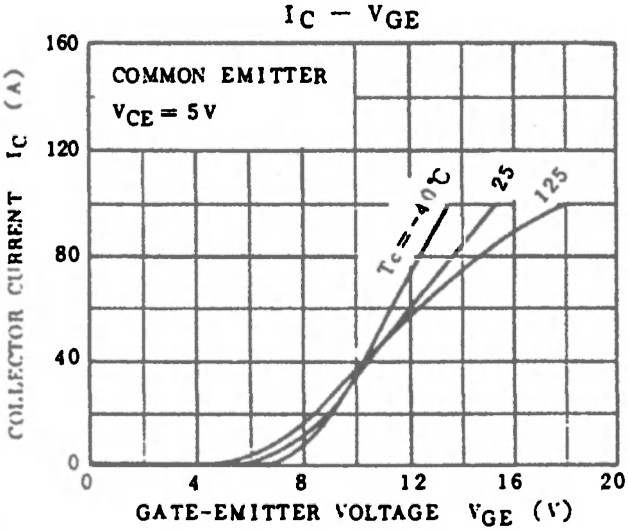

$V_{CE}, V_{GE} - Q_G$

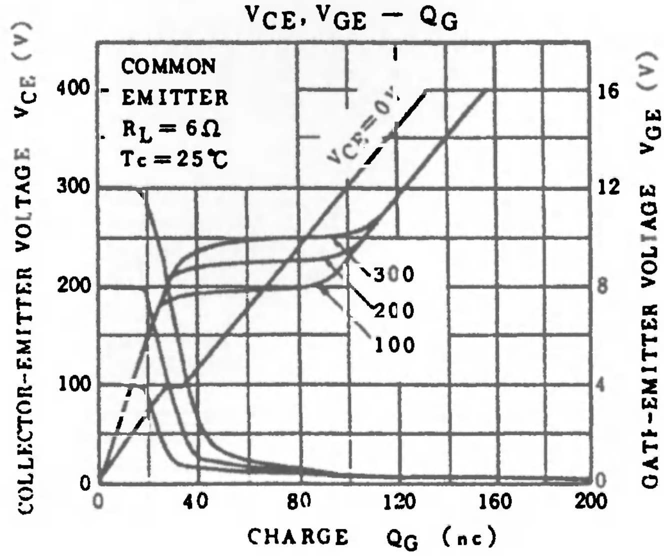

PC817 Series

High Density Mounting Type Photocoupler

✽ Lead forming type (I type) and taping reel type (P type) are also available. (**PC817I/PC817P**)
✽✽ TUV (VDE0884) approved type is also available as an option.

■ Features

1. Current transfer ratio (CTR: MIN. 50% at I_F = 5mA, V_{CE}=5V)
2. High isolation voltage between input and output (V_{iso} : 5 000V_{rms})
3. Compact dual-in-line package
   - **PC817** : 1-channel type
   - **PC827** : 2-channel type
   - **PC837** : 3-channel type
   - **PC847** : 4-channel type
4. Recognized by UL, file No. E64380

■ Applications

1. Computer terminals
2. System appliances, measuring instruments
3. Registers, copiers, automatic vending machines
4. Electric home appliances, such as fan heaters, etc.
5. Signal transmission between circuits of different potentials and impedances

■ Outline Dimensions

(Unit : mm)

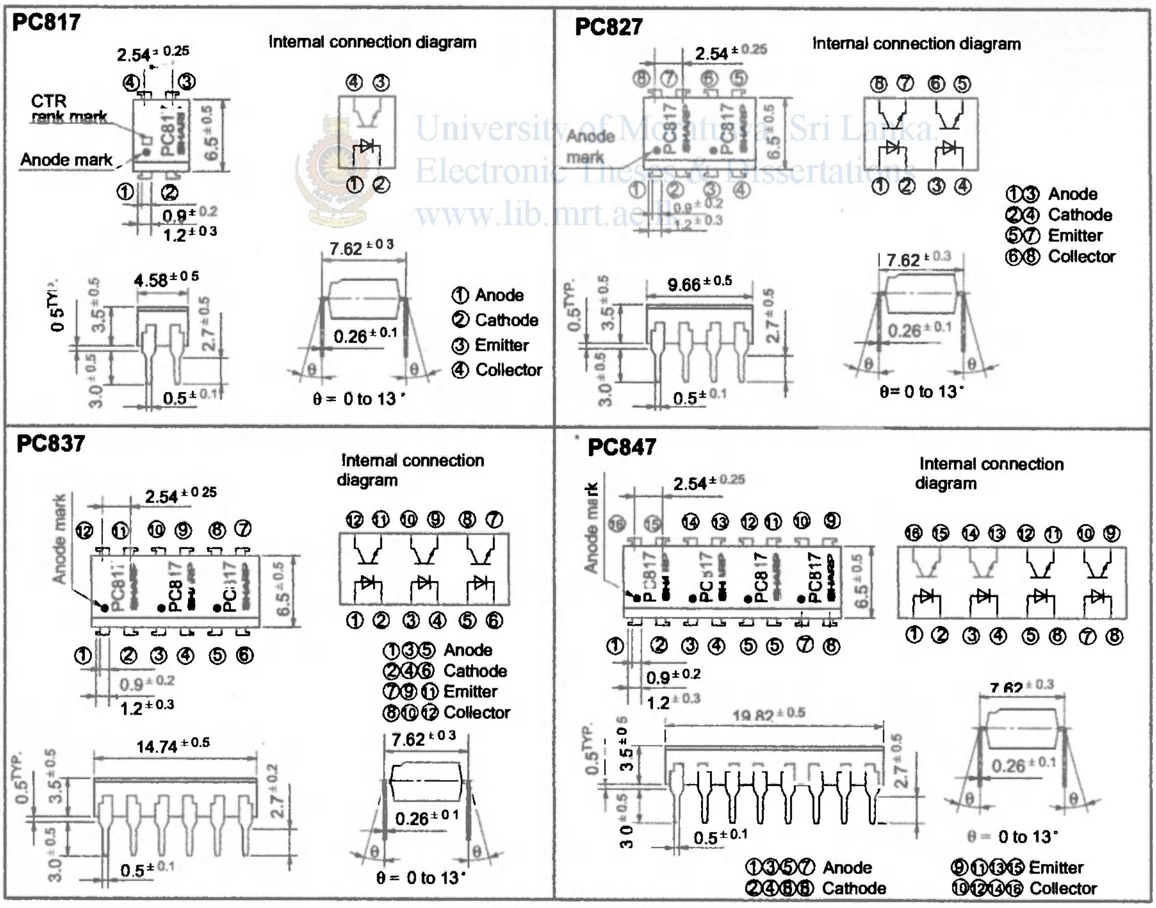

Absolute Maximum Ratings (Ta= 25°C)

	Parameter	Symbol	Rating	Unit
Input	Forward current	I_F	50	mA
	*1 Peak forward current	I_{FM}	1	A
	Reverse voltage	V_R	6	V
	Power dissipation	P	70	mW
Output	Collector-emitter voltage	V_{CEO}	35	V
	Emitter-collector voltage	V_{ECO}	6	V
	Collector current	I_C	50	mA
	Collector power dissipation	P_C	150	mW
	Total power dissipation	P_{tot}	200	mW
	*2 Isolation voltage	V_{iso}	5 000	V_{rms}
	Operating temperature	T_{opr}	- 30 to + 100	°C
	Storage temperature	T_{stg}	- 55 to + 125	°C
	*3 Soldering temperature	T_{sol}	260	°C

*1 Pulse width<=100μs, Duty ratio : 0.001
*2 40 to 60% RH, AC for 1 minute
*3 For 10 seconds

Electro-optical Characteristics (Ta= 25°C)

	Parameter	Symbol	Conditions	MIN.	TYP.	MAX.	Unit
Input	Forward voltage	V_F	I_F = 20mA	-	1.2	1.4	V
	Peak forward voltage	V_{FM}	I_{FM} = 0.5A	-	-	3.0	V
	Reverse current	I_R	V_R = 4V	-	-	10	μA
	Terminal capacitance	C_t	V= 0, f= 1kHz	-	30	250	pF
Output	Collector dark current	I_{CEO}	V_{CE} = 20V	-	-	10^{-7}	A
Transfer charac-teristics	*4 Current transfer ratio	CTR	I_F = 5mA, V_{CE} = 5V	50	-	600	%
	Collector-emitter saturation voltage	$V_{CE(sat)}$	I_F = 20mA, I_C = 1mA	-	0.1	0.2	V
	Isolation resistance	R_{ISO}	DC500V, 40 to 60% RH	5 x 10^{10}	10^{11}	-	Ω
	Floating capacitance	C_f	V= 0, f= 1MHz	-	0.6	1.0	pF
	Cut-off frequency	f_c	V_{CE} = 5V, I_C = 2mA, R_L = 100Ω, - 3dB	-	80	-	kHz
	Response time – Rise time	t_r	V_{CE} = 2V, I_C = 2mA, R_L = 100Ω	-	4	18	μs
	Response time – Fall time	t_f	V_{CE} = 2V, I_C = 2mA, R_L = 100Ω	-	3	18	μs

*4 Classification table of current transfer ratio is shown below.

Model No.	Rank mark	CTR (%)
PC817A	A	80 to 160
PC817B	B	130 to 260
PC817C	C	200 to 400
PC817D	D	300 to 600
PC8●7AB	A or B	80 to 260
PC8●7BC	B or C	130 to 400
PC8●7CD	C or D	200 to 600
PC8●7AC	A, B or C	80 to 400
PC8●7BD	B, C or D	130 to 600
PC8●7AD	A, B, C or D	80 to 600
PC8●7	A, B, C, D or No mark	50 to 600

● : 1 or 2 or 3 or 4

Fig. 1 Forward Current vs. Ambient Temperature

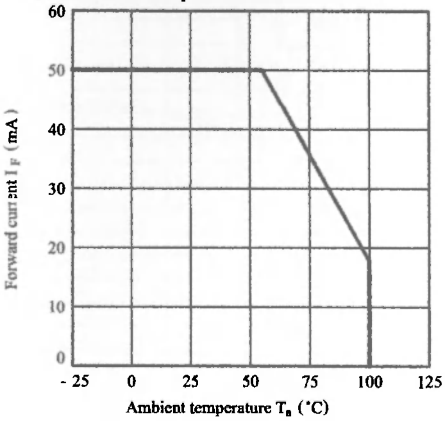

Fig. 2 Collector Power Dissipation vs. Ambient Temperature

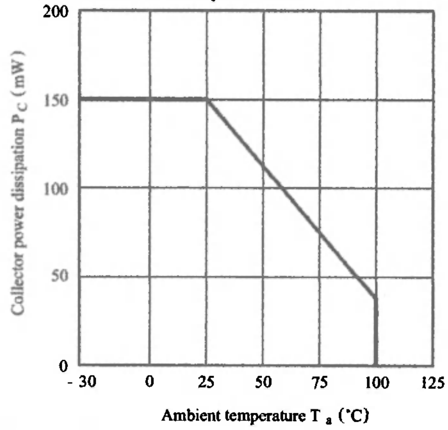

Fig. 3 Peak Forward Current vs. Duty Ratio

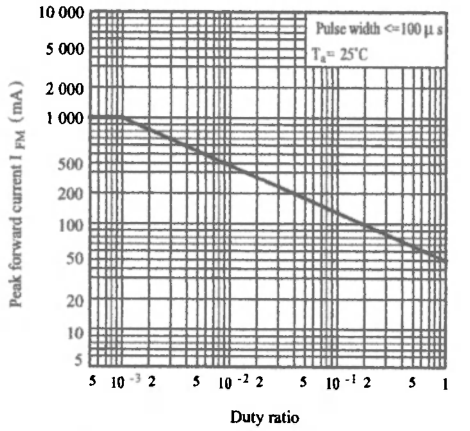

Fig. 4 Current Transfer Ratio vs. Forward Current

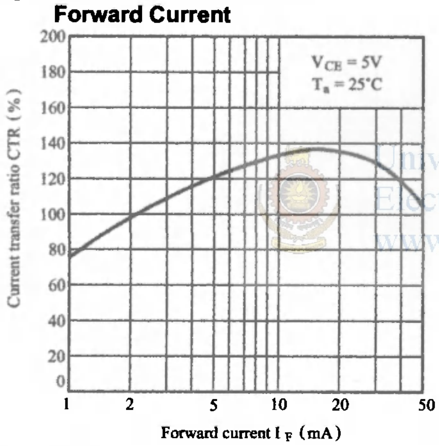

Fig. 5 Forward Current vs. Forward Voltage

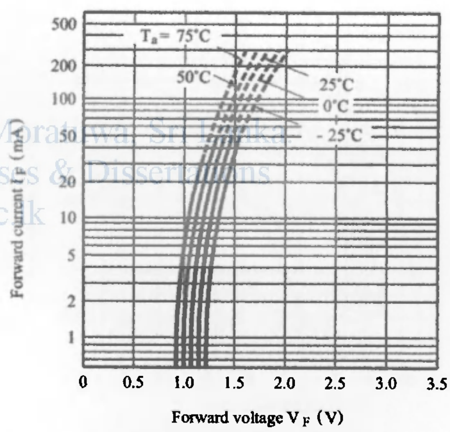

Fig. 6 Collector Current vs. Collector-emitter Voltage

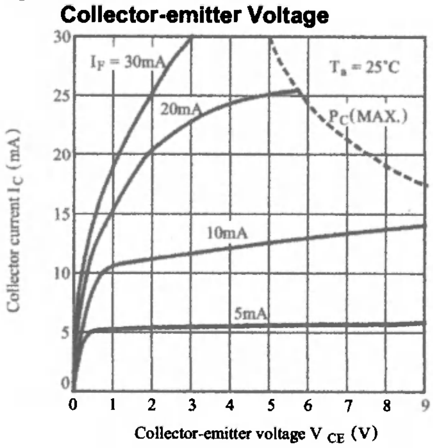

Fig. 7 Relative Current Transfer Ratio vs. Ambient Temperature

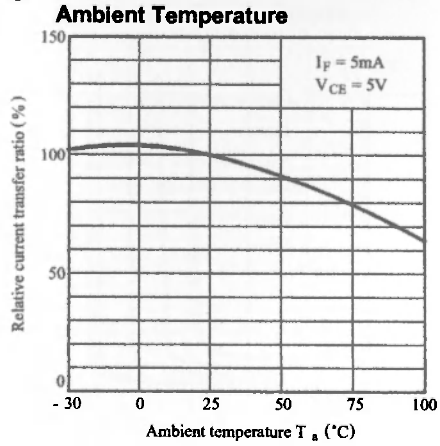

Fig. 8 Collector-emitter Saturation Voltage vs. Ambient Temperature

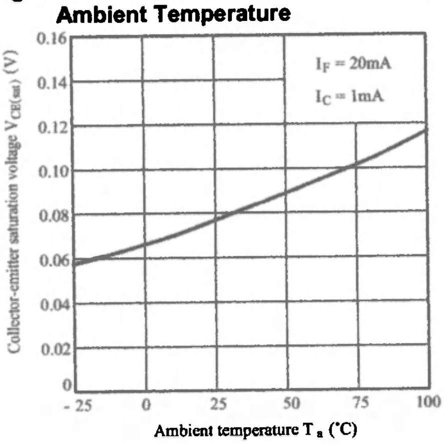

Fig. 9 Collector Dark Current vs. Ambient Temperature

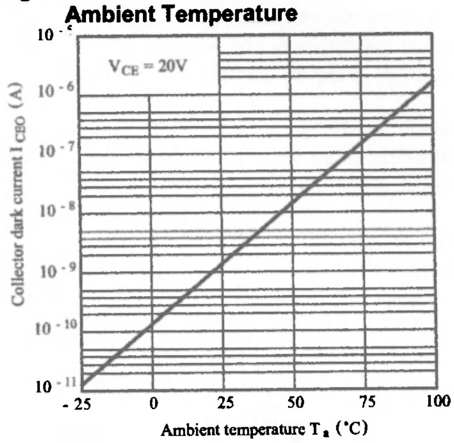

Fig.10 Response Time vs. Load Resistance

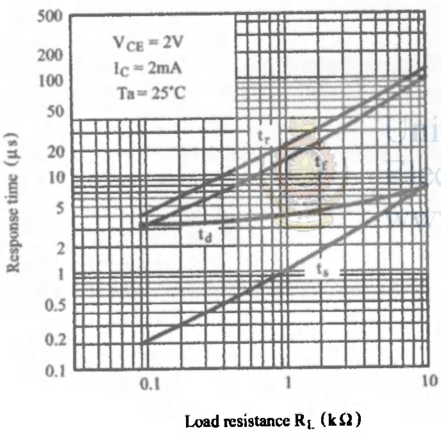

Fig.11 Frequency Response

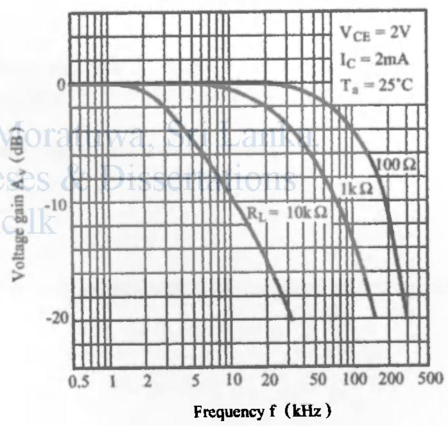

Test Circuit for Response Time

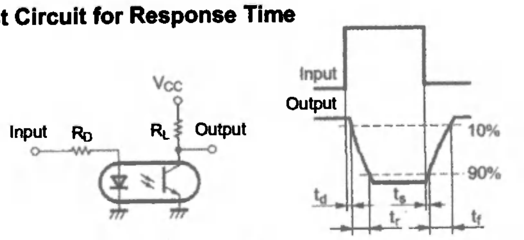

Fig.12 Collector-emitter Saturation Voltage vs. Forward Current

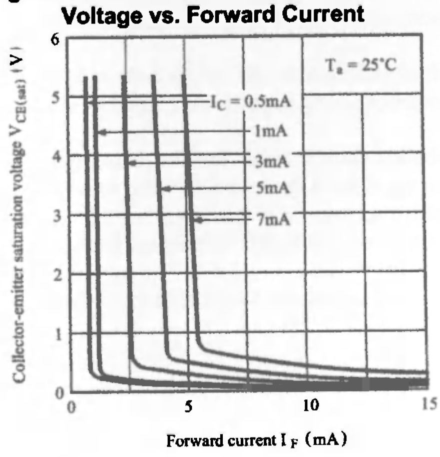

Test Circuit for Frepuency Response

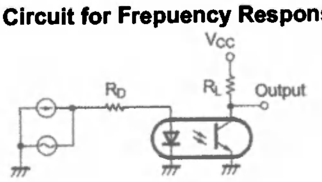

● Please refer to the chapter "Precautions for Use"

NOTICE

- The circuit application examples in this publication are provided to explain representative applications of SHARP devices and are not intended to guarantee any circuit design or license any intellectual property rights. SHARP takes no responsibility for any problems related to any intellectual property right of a third party resulting from the use of SHARP's devices.
- Contact SHARP in order to obtain the latest device specification sheets before using any SHARP device. SHARP reserves the right to make changes in the specifications, characteristics, data, materials, structure, and other contents described herein at any time without notice in order to improve design or reliability. Manufacturing locations are also subject to change without notice.
- Observe the following points when using any devices in this publication. SHARP takes no responsibility for damage caused by improper use of the devices which does not meet the conditions and absolute maximum ratings to be used specified in the relevant specification sheet nor meet the following conditions:

(i) The devices in this publication are designed for use in general electronic equipment designs such as:
– Personal computers
– Office automation equipment
– Telecommunication equipment [terminal]
– Test and measurement equipment
– Industrial control
– Audio visual equipment
– Consumer electronics

(ii) Measures such as fail-safe function and redundant design should be taken to ensure reliability and safety when SHARP devices are used for or in connection with equipment that requires higher reliability such as:
– Transportation control and safety equipment (i.e., aircraft, trains, automobiles, etc.)
– Traffic signals
– Gas leakage sensor breakers
– Alarm equipment
– Various safety devices, etc.

(iii) SHARP devices shall not be used for or in connection with equipment that requires an extremely high level of reliability and safety such as:
– Space applications
– Telecommunication equipment [trunk lines]
– Nuclear power control equipment
– Medical and other life support equipment (e.g., scuba).

- Contact a SHARP representative in advance when intending to use SHARP devices for any "specific" applications other than those recommended by SHARP or when it is unclear which category mentioned above controls the intended use.
- If the SHARP devices listed in this publication fall within the scope of strategic products described in the Foreign Exchange and Foreign Trade Control Law of Japan, it is necessary to obtain approval to export such SHARP devices.
-
- Contact and consult with a SHARP representative if there are any questions about the contents of this publication.

Appendix 5.

UTC D313 NPN EPITAXIAL PLANAR TRANSISTOR

NPN EPITAXIAL PLANAR TRANSISTOR

DESCRIPTION

The UTC D313 is designed for use in general purpose amplifier and switching applications.

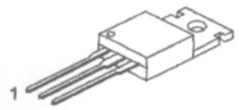

TO-220

1:BASE 2:COLLECTOR 3:EMITTER

ABSOLUTE MAXIMUM RATINGS

PARAMETER	SYMBOL	VALUE	UNIT
Collector-Base Voltage	VCBO	60	V
Collector-Emitter Voltage	VCEO	60	V
Emitter-Base Voltage	VEBO	5	V
Collector Current	Ic	3	A
Storage Temperature	T_{STG}	-55 ~ +150	°C
Junction Temperature	Tj	150	°C

ELECTRICAL CHARACTERISTICS(Ta=25°C)

PARAMETER	SYMBOL	TEST CONDITIONS	MIN	TYP	MAX	UNIT
Collector-Base Breakdown Voltage	BVCBO	IC=1mA	60			V
Collector-Emitter Breakdown Voltage	BVCEO	IC=10mA	60			V
Emitter-Base Breakdown Voltage	BVEBO	IE=100uA	5			V
Collector Cut-Off Current	ICBO	VCB=20V, IE=0			0.1	mA
Emitter Cut-Off Current	IEBO	VEB=4V, IC=0			1.0	mA
Collector-Emitter Saturation Voltage	VCE(SAT)	IC=2A, IB=0.2A			1.0	V
Base-Emitter On voltage	VBE(ON)	VCE=2V, IC=1A			1.5	V
DC Current Gain	hFE	IC=1A, VCE=2V IC=0.1A,VCE=2V	40 40		320	

CLASSIFICATION ON hFE

RANK	C	D	E	F
RANGE	40-80	60-120	100-200	160-320

DC CURRENT GAINT

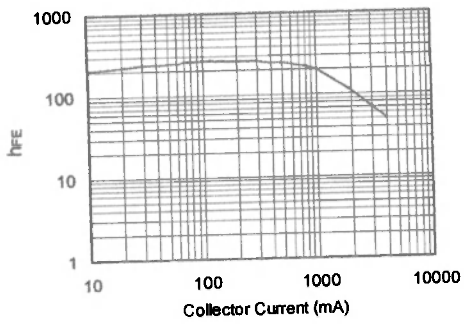

SATURATION VOLTAGE v.s. COLLECTOR CURRENT

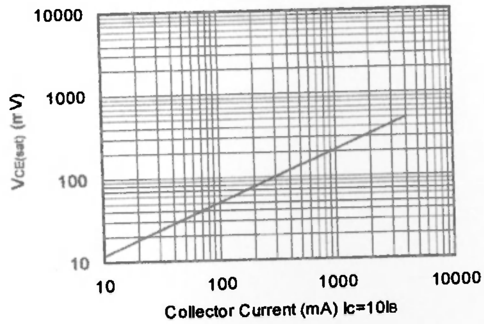

VBE(SAT) v.s.Ic

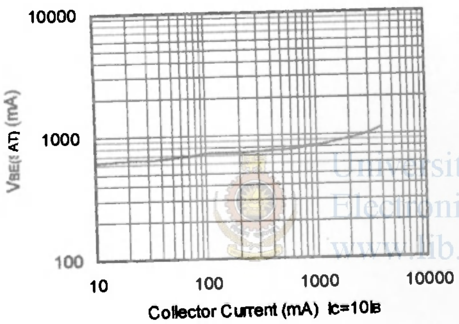

SOA

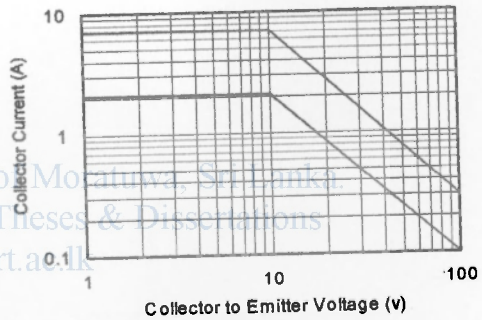

VBE(ON) v.s. Ic

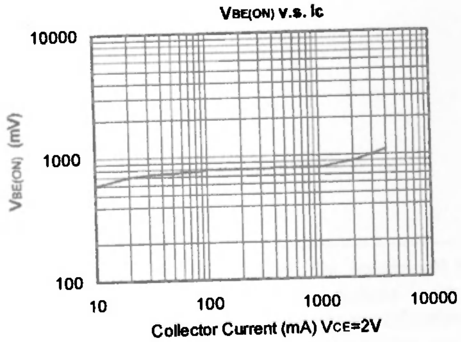

SDLS046

SN5413, SN54LS13, SN7413, SN74LS13 DUAL 4-INPUT POSITIVE-NAND SCHMITT TRIGGERS

DECEMBER 1983 – REVISED MARCH 1988

- **Operation from Very Slow Edges**
- **Improved Line-Receiving Characteristics**
- **High Noise Immunity**

SN5413, SN54LS13 . . . J OR W PACKAGE
SN7413 . . . N PACKAGE
SN74LS13 . . . D OR N PACKAGE
(TOP VIEW)

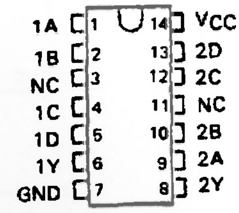

SN54LS13 . . . FK PACKAGE
(TOP VIEW)

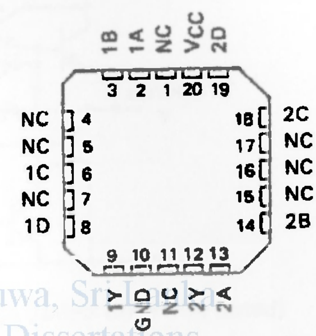

NC – No internal connection

description

Each circuit functions as a 4-input NAND gate, but because of the Schmitt action, it has different input threshold levels for positive (V_{T+}) and for negative going (V_{T-}) signals.

These circuits are temperature-compensated and can be triggered from the slowest of input ramps and still give clean, jitter-free output signals.

The SN5413 and SN54LS13 are characterized for operation over the full military temperature range of -55°C to 125°C. The SN7413 and SN74LS13 are characterized for operation from 0°C to 70°C.

logic symbol†

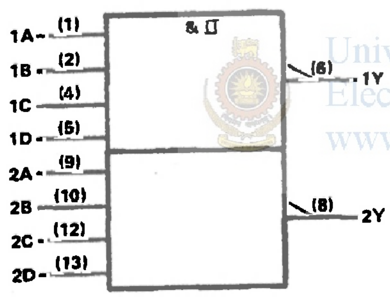

† This symbol is in accordance with ANSI/IEEE Std 91-1984 and IEC Publication 617-13.
Pin numbers shown are for D, J, N, and W packages.

logic diagram (positive logic)

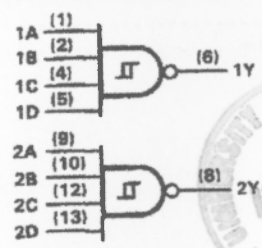

$Y = \overline{ABCD}$

SN5413, SN54LS13, SN7413, SN74LS13
DUAL 4-INPUT
POSITIVE-NAND SCHMITT TRIGGERS

schematics

'13

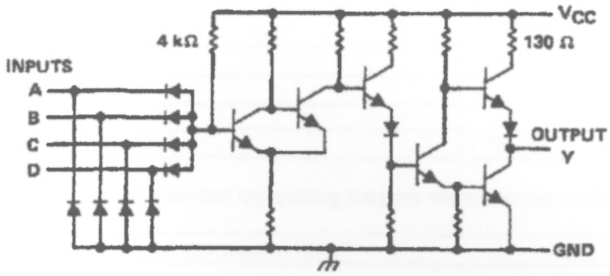

'LS13

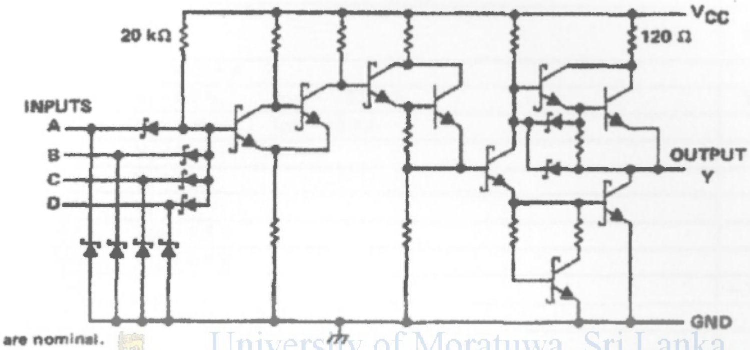

Resistor values are nominal.

absolute maximum ratings over operating free-air temperature range (unless otherwise noted)

Supply voltage, V_{CC} (see Note 1)		7 V
Input voltage:	'13	5.5 V
	'LS13	7 V
Operating free-air temperature:	SN54'	−55°C to 125°C
	SN74'	0°C to 70°C
Storage temperature range		−65°C to 150°C

NOTE 1: Voltage values are with respect to network ground terminal.

recommended operating conditions

		SN5413			SN7413			UNIT
		MIN	NOM	MAX	MIN	NOM	MAX	
V_{CC}	Supply voltage	4.5	5	5.5	4.75	5	5.25	V
I_{OH}	High-level output current			−0.8			−0.8	mA
I_{OL}	Low-level output current			16			16	mA
T_A	Operating free-air temperature	−55		125	0		70	°C

electrical characteristics over recommended operating free-air temperature range (unless otherwise noted)

PARAMETER	TEST CONDITIONS†			MIN	TYP‡	MAX	UNIT
V_{T+}	V_{CC} = 5 V			1.5	1.7	2	V
V_{T-}	V_{CC} = 5 V			0.6	0.9	1.1	V
Hysteresis ($V_{T+} - V_{T-}$)	V_{CC} = 5 V			0.4	0.8		V
V_{IK}	V_{CC} = MIN,	I_I = −12 mA				−1.5	V
V_{OH}	V_{CC} = MIN,	V_I = 0.6 V,	I_{OH} = −0.8 mA	2.4	3.4		V
V_{OL}	V_{CC} = MIN,	V_I = 2 V,	I_{OL} = 16 mA		0.2	0.4	V
I_{T+}	V_{CC} = 5 V,	$V_I = V_{T+}$			−0.65		mA
I_{T-}	V_{CC} = 5 V,	$V_I = V_{T-}$			−0.85		mA
I_I	V_{CC} = MAX,	V_I = 5.5 V				1	mA
I_{IH}	V_{CC} = MAX,	V_{IH} = 2.4 V				40	μA
I_{IL}	V_{CC} = MAX,	V_{IL} = 0.4 V			−1	−1.6	mA
I_{OS}§	V_{CC} = MAX,			−18		−55	mA
I_{CCH}	V_{CC} = MAX				14	23	mA
I_{CCL}	V_{CC} = MAX				20	32	mA

† For conditions shown as MIN or MAX, use the appropriate value specified under recommended operating conditions.
‡ All typical values are at V_{CC} = 5 V, T_A = 25°C.
§ Not more than one output should be shorted at a time.

switching characteristics, V_{CC} = 5 V, T_A = 25°C

PARAMETER	FROM (INPUT)	TO (OUTPUT)	TEST CONDITIONS		MIN	TYP	MAX	UNIT
t_{PLH}	Any	Y	R_L = 400 Ω,	C_L = 15 pF		18	27	ns
t_{PHL}						15	22	ns

SN54LS13, SN74LS13
DUAL 4-INPUT
POSITIVE-NAND SCHMITT TRIGGERS

recommended operating conditions

		SN54LS13			SN74LS13			UNIT
		MIN	NOM	MAX	MIN	NOM	MAX	
V_{CC}	Supply voltage	4.5	5	5.5	4.75	5	5.25	V
I_{OH}	High-level output current			– 0.4			– 0.4	mA
I_{OL}	Low-level output current			4			8	mA
T_A	Operating free-air temperature	– 55		125	0		70	°C

electrical characteristics over recommended operating free-air temperature range (unless otherwise noted)

PARAMETER	TEST CONDITIONS†				SN54LS13			SN74LS13			UNIT
					MIN	TYP‡	MAX	MIN	TYP‡	MAX	
V_{T+}	V_{CC} = 5 V				1.4	1.6	1.9	1.4	1.6	1.9	V
V_{T-}	V_{CC} = 5 V				0.5	0.8	1	0.5	0.8	1	V
Hysteresis ($V_{T+} - V_{T-}$)	V_{CC} = 5 V				0.4	0.8		0.4	0.8		V
V_{IK}	V_{CC} = MIN,	I_I = – 18 mA					– 1.5			– 1.5	V
V_{OH}	V_{CC} = MIN,	V_I = 0.5 V,	I_{OH} = – 0.4 mA		2.5	3.4		2.7	3.4		V
V_{OL}	V_{CC} = MIN,	V_I = 1.9 V		I_{OL} = 4 mA		0.25	0.4		0.25	0.4	V
				I_{OL} = 8 mA					0.35	0.5	
I_{T+}	V_{CC} = 5 V,	$V_I = V_{T+}$				– 0.14			– 0.14		mA
I_{T-}	V_{CC} = 5 V,	$V_I = V_{T-}$				– 0.18			– 0.18		mA
I_I	V_{CC} = MAX,	V_I = 7 V					0.1			0.1	mA
I_{IH}	V_{CC} = MAX,	V_{IH} = 2.7 V					20			20	µA
I_{IL}	V_{CC} = MAX,	V_{IL} = 0.4 V					– 0.4			– 0.4	mA
I_{OS}§	V_{CC} = MAX				– 20		– 100	– 20		– 100	mA
I_{CCH}	V_{CC} = MAX					2.9	6		2.9	6	mA
I_{CCL}	V_{CC} = MAX					4.1	7		4.1	7	mA

† For conditions shown as MIN or MAX, use the appropriate value specified under recommended operating conditions.
‡ All typical values are at V_{CC} = 5 V, T_A = 25°C.
§ Not more than one output should be shorted at a time, and duration of the short-circuit should not exceed one second.

switching characteristics, V_{CC} = 5 V, T_A = 25°C

PARAMETER	FROM (INPUT)	TO (OUTPUT)	TEST CONDITIONS		MIN	TYP	MAX	UNIT
t_{PLH}	Any	Y	R_L = 2 kΩ,	C_L = 15 pF		15	22	ns
t_{PHL}						18	27	ns

PARAMETER MEASUREMENT INFORMATION

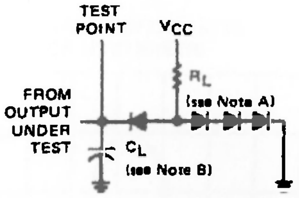

LOAD CIRCUIT

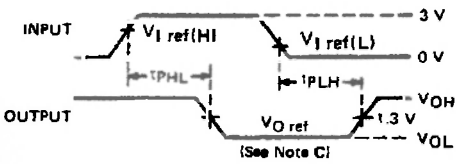

VOLTAGE WAVEFORMS

NOTES: A. All diodes are 1N3064 or equivalent.
B. C_L includes probe and jig capacitance.
C. Generator characteristics and reference voltages are:

	Generator Characteristics				Reference Voltages		
	Z_{out}	PRR	t_r	t_f	$V_{I\,ref(H)}$	$V_{I\,ref(L)}$	$V_{O\,ref}$
SN54'/SN74'	50 Ω	1 MHz	10 ns	10 ns	1.7 V	0.9 V	1.5 V
SN54LS'/SN74LS'	50 Ω	1 MHz	15 ns	6 ns	1.6 V	0.8 V	1.3 V

TYPICAL CHARACTERISTICS OF '13 CIRCUITS

POSITIVE-GOING THRESHOLD VOLTAGE
vs
FREE-AIR TEMPERATURE

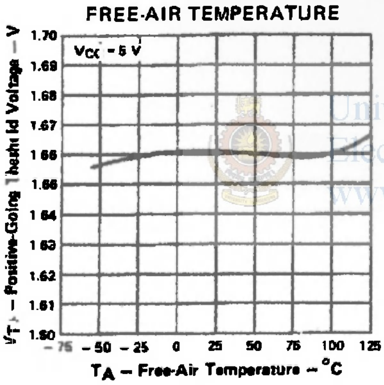

FIGURE 1

NEGATIVE-GOING THRESHOLD VOLTAGE
vs
FREE-AIR TEMPERATURE

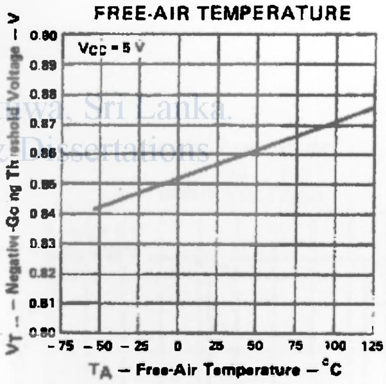

FIGURE 2

HYSTERESIS
vs
FREE-AIR TEMPERATURE

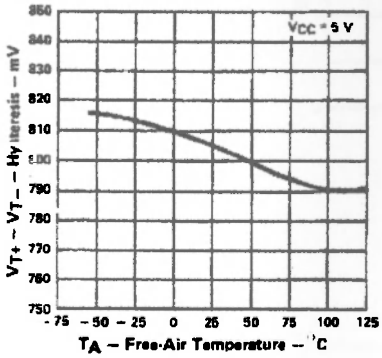

FIGURE 3

Data for temperatures below 0°C and 70°C and supply voltages below 4.75 V and above 5.25 V are applicable for SN5413 only.

TYPICAL CHARACTERISTICS OF '13 CIRCUITS

DISTRIBUTION OF UNITS
FOR HYSTERESIS

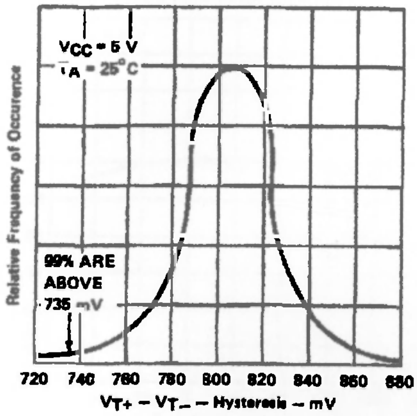

FIGURE 4

THRESHOLD VOLTAGES
vs
SUPPLY VOLTAGE

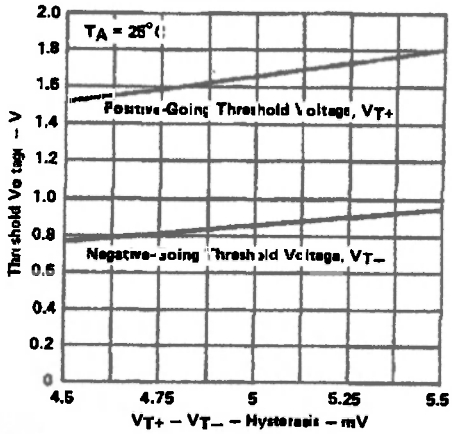

FIGURE 5

HYSTERESIS
vs
SUPPLY VOLTAGE

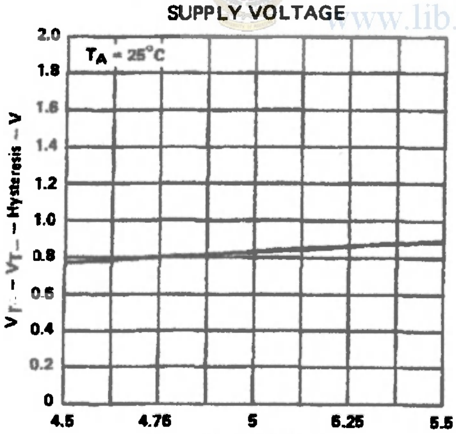

FIGURE 6

OUTPUT VOLTAGE
vs
INPUT VOLTAGE

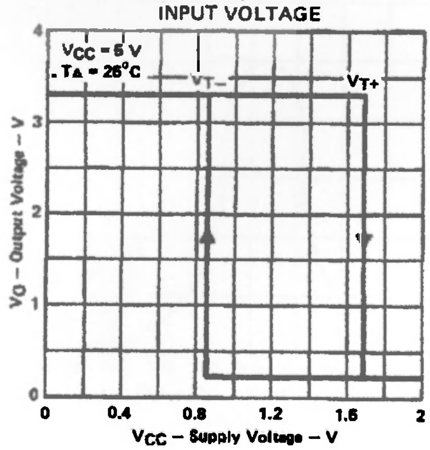

FIGURE 7

Data for temperatures below 0°C and 70°C and supply voltages below 4.75 V and above 5.25 V are applicable for SN5413 only.

TYPICAL CHARACTERISTICS OF 'LS13 CIRCUITS

POSITIVE-GOING THRESHOLD VOLTAGE
vs
FREE-AIR TEMPERATURE

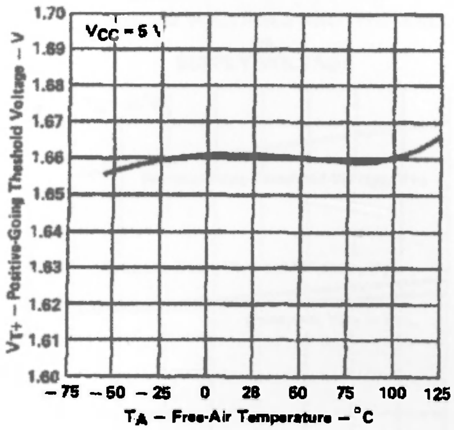

FIGURE 8

NEGATIVE-GOING THRESHOLD VOLTAGE
vs
FREE-AIR TEMPERATURE

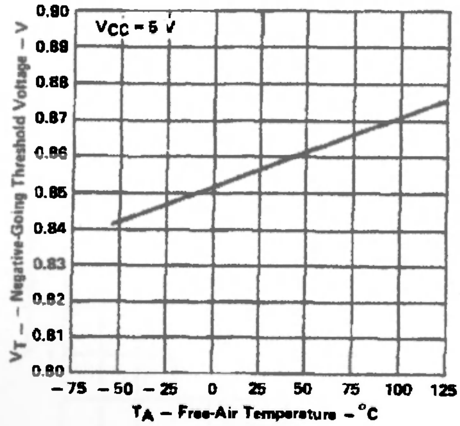

FIGURE 9

HYSTERESIS
vs
FREE-AIR TEMPERATURE

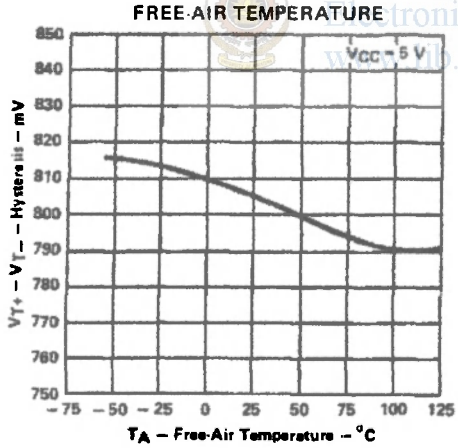

FIGURE 10

DISTRIBUTION OF UNITS
FOR HYSTERESIS

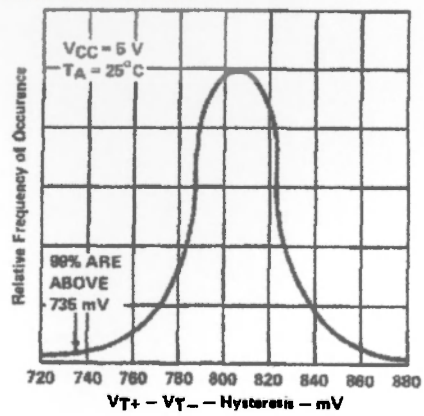

FIGURE 11

Data for temperatures below 0°C and above 70°C and supply voltages below 4.75 V and above 5.25 V are applicable for SN54LS13 only.

TYPICAL CHARACTERISTICS OF 'LS13 CIRCUITS

THRESHOLD VOLTAGES AND HYSTERESIS
vs
SUPPLY VOLTAGE

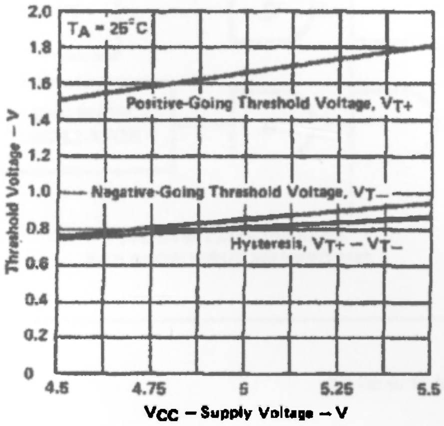

FIGURE 12

OUTPUT VOLTAGE
vs
INPUT VOLTAGE

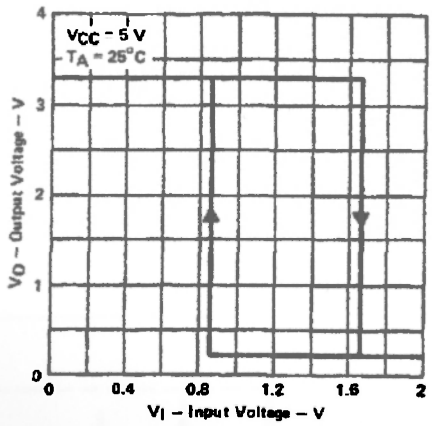

FIGURE 13

Data for temperatures below 0°C and above 70°C and supply voltages below 4.75 V and above 5.25 V are applicable for SN54LS13 only.

TYPICAL APPLICATION DATA

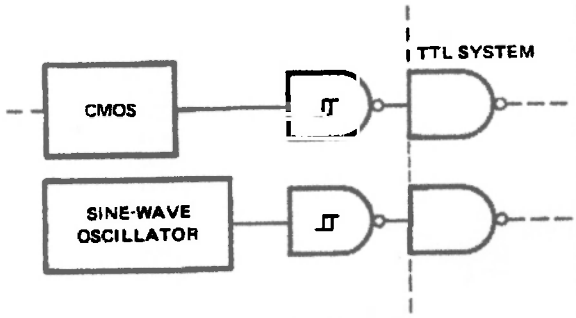

TTL SYSTEM INTERFACE
FOR SLOW INPUT WAVEFORMS

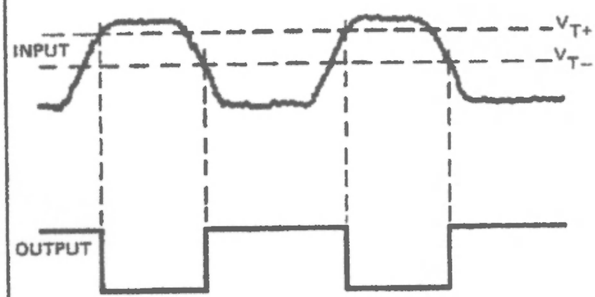

PULSE SHAPER

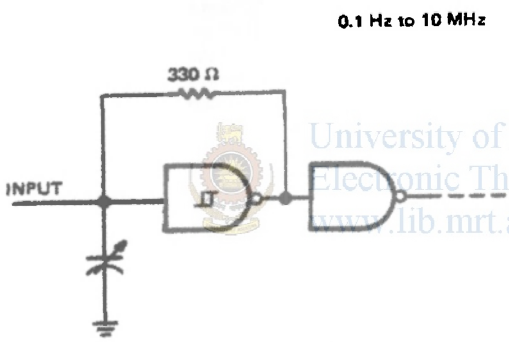

MULTIVIBRATOR

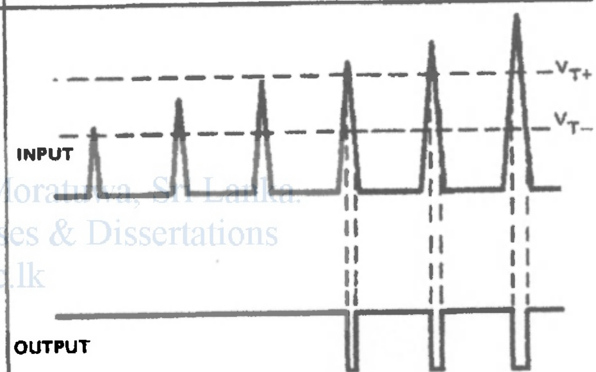

THRESHOLD DETECTOR

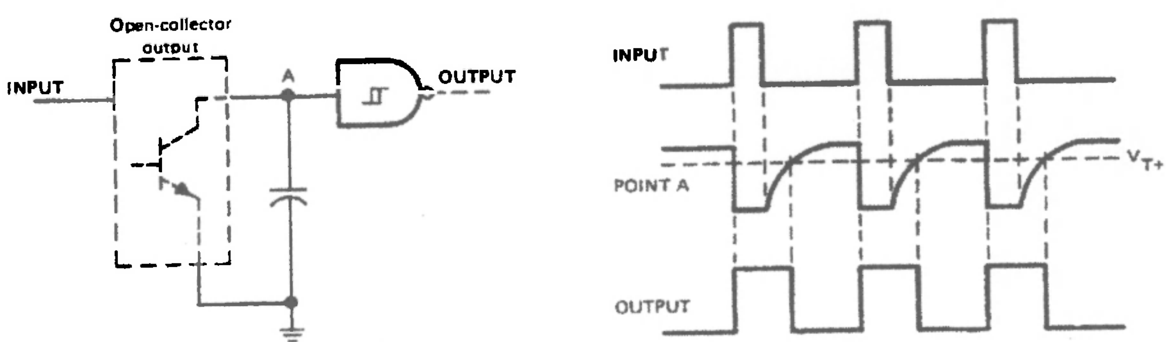

PULSE STRETCHER

Appendix 7.

MICROPROCESSOR PROGRAM FOR 'PI' CONTROLLER STRATEGY II

```
 __config _LVP_OFF & _XT_OSC & _WDT_OFF & _PWRTE_ON & _CP_OFF & _BODEN_OFF & _DEBUG_OFF

; for PID
        list p=16F877A
        #include p16F877a.inc

        cblock  0x40
        CEBPulselengthH
        CEBPulselengthL
        GENPulselengthH
        GENPulselengthL
        errorL
        errorH
        errorfrequ
        INT_TERM_H
        INT_TERM_L
        PROP_TERM_H
        PROP_TERM_L
        PID_RES_H
        PID_RES_L
        PWM
        flags                   ;0-low frequency 1-error neg 2-cal over 3-start new cycle
                                        ;4-gen ok 5-ceb ok
        endc

AARGB0          equ 0x50
AARGB1          equ 0x51
AARGB5          equ 0x52
BARGB0          equ 0x53
BARGB1          equ 0x54
REMB0           equ 0x55
REMB1           equ 0x56
TEMP            equ 0x57
LOOPCOUNT       equ 0x58
TEMP2           equ 0x59
        org     0x00
        goto    start

        org     0x04
        banksel         INTCON
        bcf                     INTCON,0
        btfss           INTCON,2
;       goto            chk_low_freq
        retfie
        bcf                     INTCON,2
        banksel flags
        btfss           flags,4     ;chk gen ok
        goto            setlowfreq
        btfsc           flags,5
        goto            setoutput
        banksel flags
        bsf                     flags,0
        bsf                     flags,3
        goto            setoutput
setlowfreq
        banksel flags
        bsf                     flags,0
        bsf                     flags,3
        call            calculate
        retfie

setoutput
        call            calculate
        banksel flags
        bsf                     flags,3
;chk_low_freq
;       banksel PIR1
;       btfss   PIR1,0
;       retfie
;       Banksel flags
```

```
;		bsf		flags,0 ; low frequency or
		retfie

start

configprocessor
		banksel	PR2
		movlw	0xC7 ;199
		movwf	PR2
		banksel CCPR1L
		movlw	0x00  ;at initilize 0
		movwf	CCPR1L
		bcf	CCP1CON,CCP1X
		bcf	CCP1CON,CCP1Y
		banksel	TRISC
		bcf		TRISC,2
		banksel	T2CON
		movlw	b'00000100'   ; TMR2 = on, prescale = 1:1
		movwf	T2CON
		banksel	CCP1CON
		movlw	b'00001111'  ; and enable PWM mode
		movwf	CCP1CON

		banksel TRISB			; bit 5 for desable CEB reading
		movfw	b'11100000'  ;B,7  B,6  and B,5 are  input
		banksel	INTCON
		bsf		INTCON,7
		bsf		INTCON,6
		bsf		INTCON,5
		banksel	T1CON
		bcf		T1CON,4
		bcf		T1CON,5  ;PS 1:1  min Fz=16Hz
		BSF		STATUS, RP0
		CLRF	PIE1
		bcf		PIE1,0	; timer 1 interupt enable desabled
		BCF		STATUS, RP0
		CLRF	PIR1

		banksel	OPTION_REG
		bcf		OPTION_REG,5
		bcf		OPTION_REG,3
		bsf		OPTION_REG,0
		bsf		OPTION_REG,1
		bsf		OPTION_REG,2
		banksel	INTCON
		bsf		INTCON,7
;		bsf		INTCON,6
		bsf		INTCON,5
		bcf			INTCON,2

		banksel		INT_TERM_H
		clrf		INT_TERM_H
		clrf		INT_TERM_L
		clrf			flags
		call	setdefoultpwm


main
		Banksel	flags
		btfsc	flags,4
		goto	gen_read_ok


		clrf	flags ; new cycle
		banksel	TMR0
		clrf	TMR0
		banksel	OPTION_REG
		bsf		OPTION_REG,0	;
		bsf		OPTION_REG,1	;
		bsf		OPTION_REG,2	;timer0 ps= 1:256

		call	readGEN
		banksel	PIR1
		btfss	PIR1,0		;check if the timer 1>60ms
		goto	$+6
```

```
        Banksel flags
        bsf             flags,0 ; low frequency flag
        bcf             PIR1,0
        goto    setdefoultpwm           ; goto set defoult pwm
gen_read_ok
        nop
        nop
        call    readCEB
        btfsc           flags,2
        bcf                     flags,2

        btfsc   flags,3
        goto    main
        goto    $-2

        goto main


readCEB
        Banksel flags
        bcf             flags,3 ; ; flag for new cycle
        banksel PORTB
        btfsc   PORTB,5
        goto    CEB_freq_set
        banksel TMR1H
        CLRF    TMR1H
        CLRF    TMR1L
        banksel CEBPulselengthH
        clrf    CEBPulselengthH
        clrf    CEBPulselengthL
        banksel PORTB
        btfsc   flags,3
        goto    main
        btfsc   PORTB,7
        goto    $-3
        btfsc   flags,3
        goto    main
        btfss   PORTB,7
        goto    $-3
        BSF             T1CON, TMR1ON
        btfsc   flags,3
        goto    main
        btfsc   PORTB,7
        goto    $-3
        btfsc   flags,3
        goto    main
        btfss   PORTB,7
        goto    $-3
        BcF             T1CON, TMR1ON
        banksel TMR1H
        movfw   TMR1H
        banksel CEBPulselengthH
        movwf   CEBPulselengthH
        banksel TMR1L
        movfw   TMR1L
        banksel CEBPulselengthL
        movwf   CEBPulselengthL
        banksel flags
        bsf             flags,5
        bcf                     flags,0         ;flag for low frequency
        nop
        return

 CEB_freq_set
        movlw   0x4E
        banksel CEBPulselengthH
        movwf   CEBPulselengthH
        movlw   0x20
        banksel CEBPulselengthL
        movwf   CEBPulselengthL
        banksel flags
        bsf             flags,5
        bcf                     flags,0         ;flag for low frequency
        nop
        return
```

```
readGEN
        banksel  TMR1H
        CLRF     TMR1H
        CLRF     TMR1L
        banksel  GENPulselengthH
        clrf     GENPulselengthH
        clrf     GENPulselengthL
        banksel  PORTB

        btfsc    flags,3
        goto     main
        btfsc    PORTB,6
        goto     $-4
        btfsc    flags,3
        goto     main
        btfss    PORTB,6
        goto     $-3
        BSF              T1CON. TMR1ON
        btfsc    flags,3
        goto     main
        btfsc    PORTB,6
        goto     $-3
        btfsc    flags,3
        goto     main
        btfss    PORTB,6
        goto     $-3
        BcF              T1CON, TMR1ON
        btfsc            flags,2
        return
        banksel  TMR1H
        movfw    TMR1H
        banksel  GENPulselengthH
        movwf    GENPulselengthH
        banksel  TMR1L
        movfw    TMR1L
        banksel  GENPulselengthL
        movwf    GENPulselengthL
        banksel  flags
        bsf              flags,4
        nop
        return

calculate
TimeError ;(ceb-gen)
        btfsc    flags,0
        goto     setdefoultpwm
        banksel  GENPulselengthH
        movfw    GENPulselengthL
        subwf    CEBPulselengthL,w
        movwf    errorL
        btfsc    STATUS,0
        goto     $+5
        comf     errorL,1
        incf     errorL,0
        sublw    0xff
        movwf    errorL
        incf     GENPulselengthH,0
        goto     $+2
        movfw    GENPulselengthH
        subwf    CEBPulselengthH,w
        movwf    errorH
        btfss    STATUS,0                 ;if error is minus
        goto     setdefoultpwm        ;error minus
        nop                                                   ;error ok
errorfre
        movfw    errorH
        movwf    AARGB0
        movfw    errorL
        movwf    AARGB1
        movlw    0x08
        movwf    BARGB0
        call     UDIV1608L
        nop
```

```
		movfw	AARGB0
		addlw	0xff
		btfsc	STATUS,0
		goto	setdefoultpwm
		movfw	AARGB1
		movwf	errorfrequ

integral
		movfw	INT_TERM_H
		sublw	0x01
		btfsc	STATUS, Z
		goto	PID_add		;
		nop
		movlw	0x0A
		MOVWF	BARGB0
		CALL	UDIV1608L

;;add to previous results
		MOVF	AARGB1, W
		ADDWF	INT_TERM_L,	F
		BTFSC	STATUS, C
		INCF	INT_TERM_H,	F
		MOVF	AARGB0, W
		ADDWF	INT_TERM_H,	F
		GOTO	PID_add

;SUME_NEG
;;		BTFSS	flag,	1
;		GOTO	ADD_INT_TERM
;		MOVLW	B'00010100'
;		ADDWF	INT_TERM_H,	W
;		MOVWF	TEMP2
;		BTFSS	TEMP2,	7
;		GOTO	ADD_INT_TERM
;		GOTO	PID_add
;CHECK_2 BIG
;		MOVLW	B'11101100'
;		ADDWF	INT_TERM_H,	W
;		MOVWF	TEMP2
;		BTFSC	TEMP2,	7
;		GOTO	ADD_INT_TERM
;



PID_add
		clrf	PID_RES_H
		clrf	PID_RES_L
;set intigeal term
		movfw	INT_TERM_L;
		movwf	AARGB1
		movfw	INT_TERM_H
		movwf	AARGB0
		movlw	0x05
		MOVWF	BARGB0
		call	UDIV1608L
		movfw	AARGB1
		addwf	PID_RES_L,1
		movfw	AARGB0
		addwf	PID_RES_H,1



		clrf	AARGB0
		movfw	errorfrequ
		movwf	AARGB1
		movlw	0x02
		movwf	BARGB0
		call	UDIV1608L

		movfw	AARGB1
		movwf	AARGB0
		movlw	0x05
```

```
        movwf   BARGB0
        call    UMUL0808L

        movfw   AARGB0
        movwf   PROP_TERM_H
        movfw   AARGB1
        movwf   PROP_TERM_L

        addwf   PID_RES_L,1
        BTFSC   STATUS, C
        INCF    PID_RES_H,          F
        movfw   PROP_TERM_H
        addwf   PID_RES_H,1

        movfw   PID_RES_L
        banksel CCPR1L
        movwf   CCPR1L

        banksel flags
        bcf             flags,5
        bcf             flags,4
        return


;set_defoult_para
;       movlw   0x20
;       movwf   PWM
;       banksel CCPR1L
;       movwf   CCPR1L
;       return


;PID
;       btfsc   flags,0
;       goto    setdefoultpwm
```



```
setdefoultpwm
        banksel T2CON
        BSF             T2CON,2
        movlw   0x28  ; L= duty*2
        movwf   CCPR1L
        return


;=================div

UDIV1608L
        ;       GLOBAL          UDIV1608L
                CLRF    REMB0
        MOVLW   8
        MOVWF   LOOPCOUNT

LOOPU1608A  RLF     AARGB0,W
        RLF     REMB0, F
        MOVF    BARGB0,W
        SUBWF   REMB0, F

        BTFSC   STATUS,0
        GOTO    UOK68A
        ADDWF   REMB0, F
        BCF     STATUS,0
UOK68A  RLF     AARGB0, F

        DECFSZ  LOOPCOUNT, F
        GOTO    LOOPU1608A

        CLRF    TEMP

        MOVLW   8
```

```
        MOVWF       LOOPCOUNT

LOOPU1608B    RLF         AARGB1,W
        RLF         REMB0, F
        RLF         TEMP, F
        MOVF        BARGB0,W
        SUBWF       REMB0, F
        CLRF        AARGB5
        CLRW
        BTFSS       STATUS,0
        INCFSZ      AARGB5,W
        SUBWF       TEMP, F

        BTFSC       STATUS,0
        GOTO        UOK68B
        MOVF        BARGB0,W
        ADDWF       REMB0, F
        CLRF        AARGB5
        CLRW
        BTFSC       STATUS,0
        INCFSZ      AARGB5,W
        ADDWF       TEMP, F

        BCF         STATUS,0
UOK68B        RLF         AARGB1, F

        DECFSZ      LOOPCOUNT, F
        GOTO        LOOPU1608B
                    return
;========================================================
UMUL0808L
                    CLRF   AARGB1
        MOVLW  0x08
        MOVWF  LOOPCOUNT
        MOVF   AARGB0,W

LOOPUM0808A
        RRF    BARGB0, F
        BTFSC  STATUS,0
        GOTO   LUM0808NAP
        DECFSZ LOOPCOUNT, F
        GOTO   LOOPUM0808A

        CLRF   AARGB0
        RETLW  0x00

LUM0808NAP
        BCF    STATUS,0
        GOTO   LUM0808NA

LOOPUM0808
        RRF         BARGB0, F
        BTFSC  STATUS,0
        ADDWF  AARGB0, F
LUM0808NA     RRF    AARGB0, F
        RRF    AARGB1, F
        DECFSZ      LOOPCOUNT, F
        GOTO        LOOPUM0808
                    return
;*************************

        end
```